JACS
JOURNAL OF THE AMERICAN CHEMICAL SOCIETY
Article
Cite This: J. Am. Chem. Soc. XXXX, XXX, XXX−XXX
pubs.acs.org/JACS

Kinetics and Mechanism of Oxirane Formation by Darzens Condensation of Ketones: Quantification of the Electrophilicities of Ketones

Zhen Li, Harish Jangra, Quan Chen, Peter Mayer, Armin R. Ofial,* Hendrik Zipse,* and Herbert Mayr*

Department Chemie, Ludwig-Maximilians-Universität München, Butenandtstrasse 5-13, 81377 München, Germany

Supporting Information

ABSTRACT: The kinetics of epoxide formation by Darzens condensation of aliphatic ketones **1** with arylsulfonyl-substituted chloromethyl anions **2** ($ArSO_2CHCl^-$) have been determined photometrically in DMSO solution at 20 °C. The reactions proceed via nucleophilic attack of the carbanions at the carbonyl group to give intermediate halohydrin anions **4**, which subsequently cyclize with formation of the oxiranes **3**. Protonation of the reaction mixture obtained in THF solution at low temperature allowed the intermediates to be trapped and the corresponding halohydrins **4**-H to be isolated. Crossover experiments, i.e., deprotonation of the halohydrins **4**-H in the presence of a trapping reagent for the regenerated arylsulfonyl-substituted chloromethyl anions **2**, provided the relative rates of backward (k_{-CC}) and ring closure (k_{rc}) reactions of the intermediates. Combination of the kinetic data (k_2^{exptl}) with the splitting ratio (k_{-CC}/k_{rc}) gave the second-order rate constants k_{CC} for the attack of the carbanions **2** at the ketones **1**. These k_{CC} values and the previously reported reactivity parameters N and s_N for the arylsulfonyl-substituted chloromethyl anions **2** allowed us to use the linear free energy relationship $\log k_2(20\ °C) = s_N(N + E)$ for deriving the electrophilicity parameters E of the ketones **1** and thus predict potential nucleophilic reaction partners. Density functional theory calculations of the intrinsic reaction pathways showed that the reactions of the ketones **1** with the chloromethyl anions **2** yield two rotational isomers of the intermediate halohydrin anions **4**, only one of which can cyclize while the other undergoes retroaddition because the barrier for rotation is higher than that for reversal to the reactants **1** and **2**. The electrophilicity parameters E correlate moderately with the lowest unoccupied molecular orbital energies of the carbonyl groups, very poorly with Parr's electrophilicity indices, and best with the methyl anion affinities calculated for DMSO solution.

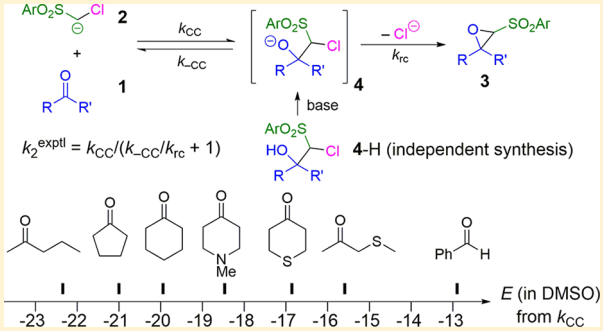

INTRODUCTION

Combinations of electrophiles with nucleophiles are the most important reactions in organic synthesis. To predict the scope and selectivities of such reactions, we have developed scales of nucleophilicity and electrophilicity on the basis of eq 1, which characterizes electrophiles by one parameter, E (electrophilicity), and nucleophiles by two solvent-dependent parameters, N (nucleophilicity) and s_N (susceptibility).[1]

$$\log k_2(20°C) = s_N(N + E) \quad (1)$$

Though carbonyl compounds belong to the most frequently employed electrophiles in organic synthesis, there has been only one previous attempt to integrate aldehydes in these scales.[2] The major problem for the quantitative determination of the electrophilic reactivities of carbonyl compounds is the fact that the nucleophilic attack at the carbonyl group is often a reversible process, which is followed by an irreversible rate-determining step.[3]

In the late 1950s, kinetic investigations of the reactions of ketones and aldehydes with sodium borohydride in protic solvents were reported by H. C. Brown.[4] Geneste and associates studied the kinetics of the reactions of ketones with BH_4^-,[5a] CN^-,[5b] SO_3^{2-},[5b,c] NH_2OH,[5b,d] and RS^-[5e] in water and reported linear correlations[5f] between the different sets of data. Thermodynamics accounts for the fact that ordinary acceptor-stabilized carbanions (e.g., malonate anions), which have previously been used as reference nucleophiles for the quantification of electrophilic reactivities,[1b,6] are not suitable for the determination of the E parameters of carbonyl compounds in aprotic solvents: Due to the high basicity of the initially formed alkoxide anions (pK_{aH} = 29.0 for MeO^- in DMSO),[7] additions of weakly basic carbanions ($pK_{aH} \approx 16$ for dimethyl malonate in DMSO)[8] to ordinary ketones and aldehydes are highly endergonic in aprotic solvents and only proceed in the presence of a suitable proton source. For that reason, reference nucleophiles are needed, which yield intermediates that undergo fast subsequent irreversible

Received: February 9, 2018

DOI: 10.1021/jacs.8b01657
J. Am. Chem. Soc. XXXX, XXX, XXX−XXX

reactions to form stable products. One possibility is to use carbanions carrying a leaving group (LG) in the α-position, since the resulting intermediates may undergo cyclization with formation of epoxides (Scheme 1).

Scheme 1. Epoxides from Carbonyl Compounds

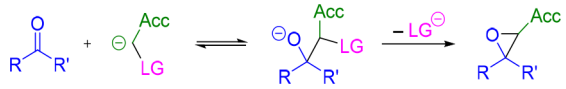

For LG = Hal, the reaction depicted in Scheme 1 corresponds to the Darzens condensation,[9,10] which has mechanistically been investigated by Ballester[11] and others.[3a,12] Whereas early work has preferentially been performed with α-halogen-substituted esters, ketones, and aldehydes (Acc = CO_2R or COR), Vogt and Tavares reported that α-halo-substituted sulfones (Acc = $ArSO_2$) also undergo the reaction sequence shown in Scheme 1 to give sulfonyl-substituted epoxides.[3b] For LG = R_2S^+, the nucleophile in Scheme 1 is a sulfonium ylide, and the sequence depicted in Scheme 1 then corresponds to the Corey–Chaykovsky epoxidation.[13,14]

In previous work, we have determined the nucleophile-specific reactivity parameters for acceptor-substituted sulfonium ylides[15] and for arylsulfonyl-substituted chloromethyl anions.[16] Since acceptor-substituted sulfonium ylides are not sufficiently nucleophilic to react with typical ketones, we have employed anions **2** (Scheme 2) as reference nucleophiles to quantify the electrophilicities of ketones.

RESULTS

Product Study. The reactions of the ketones **1a–l** with the carbanions **2a,b** in anhydrous DMSO proceeded smoothly at room temperature (Scheme 2) and gave the epoxides **3** in good yields. The asymmetric ketones **1i–l** generally reacted with low diastereoselectivity. Only in the reaction of **1l** with **2b**, the formation of the diastereomer with $ArSO_2$ and CF_3 *trans* to each other is highly preferred (de = 88%) (Scheme 2). The different stereoselectivities of **2a** and **2b** in reactions with **1l** have been observed in numerous experiments where **1l** was used as a trapping reagent in crossover experiments (see below). As shown in the Supporting Information, **2a** always gave 2/1 mixtures of two diastereomers, while **2b** gave one diastereomer almost exclusively, possibly because **1l** reacts with **2a**, but not with **2b**, under diffusion control.[17]

Kinetic Investigations. All kinetic investigations were performed in anhydrous DMSO solution at 20 °C by following the disappearance of the UV/vis absorptions of the carbanion **2a** (320 nm) or **2b** (405 nm) under pseudo-first-order conditions ($[\mathbf{1}]_0/[\mathbf{2}]_0 > 10$). As the carbanions **2a,b** decompose on the minute time scale at 20 °C (depending on the method of preparation), they were generated by treatment of their conjugate CH acids with 1.00–1.05 equiv of *t*-BuOK in dry THF at −78 °C. Small amounts of these solutions were dissolved in DMSO at 20 °C immediately before the ketones **1** were added. The first-order rate constants k_{obsd} were obtained by least-squares fitting of the exponential function $A = A_0 \exp(-k_{obsd}t) + C$ to the observed time-dependent absorbances A of **2** (Figure 1a). The slopes of the linear correlations between k_{obsd} and the different concentrations of **1a–j** (Figure

Scheme 2. Reactions of Carbanions 2 with Ketones 1 and Corresponding Gross Second-Order Rate Constants k_2^{exptl}

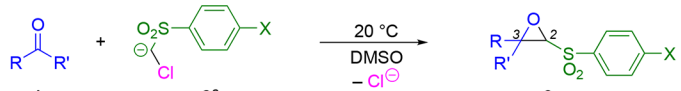

1 **2**[a] **3**

Ketones **1**		X	k_2^{exptl} (M^{-1} s^{-1})[b]	Oxiranes **3** (yield)
	**1a** n = 1	**2b** CN	7.05×10^3	**3ab** (80%)[c]
	1b n = 2	**2a** H		**3ba** (87%)[d]
		2b CN	1.31×10^2	**3bb** (73%)[d]
	1c n = 3	**2a** H	2.98×10^3	**3ca** (95%)[c]
		2b CN	2.61×10^2	**3cb** (75%)[c]
	1d n = 4	**2a** H	8.49×10^1	**3da** (90%)[c]
	**1e** X = NMe	**2a** H	1.77×10^4	**3ea** (90%)[c]
		2b CN	1.82×10^3	**3eb** (90%)[c]
	1f X = O	**2b** CN	7.62×10^3	**3fb** (70%)[c]
	1g X = S	**2a** H	very fast[e]	**3ga** (95%)[c]
		2b CN	1.81×10^4	**3gb** (85%)[c]
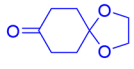	**1h**	**2a** H	2.12×10^4	**3ha** (80%)[c]
		2b CN	3.00×10^3	**3hb** (75%)[c]
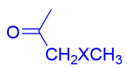	**1i** X = CH_2	**2a** H	7.42×10^1	**3ia** (90%, rel-2S,3S/rel-2R,3S = 2.6)[c]
	1j X = S	**2b** CN	3.21×10^4	**3jb** (80%, rel-2S,3S/rel-2R,3S = 2.2)[d]
	1k X = O	**2b** CN	very fast[e]	**3kb** (89%, rel-2R,3R/rel-2R,3S = 2.3)[c]
	**1l**	**2a** H	very fast[e]	**3la** (90%, rel-2R,3R/rel-2R,3S = 2.0)[c]
		2b CN	very fast[e]	**3lb** (80%, rel-2S,3S/rel-2R,3S > 15)[c]

[a]Counterion: K^+ for kinetics, Na^+ for product studies. [b]Carbanions **2a,b** generated by treatment of (**2a,b**)-H with *t*-BuOK, as described in the section "Kinetic Investigations". [c]Isolated yield obtained after chromatographic purification. [d]Yield determined by ^1H NMR spectroscopy using *m*-xylene as an internal standard. [e]Too fast to be measured by the stopped-flow technique.

DOI: 10.1021/jacs.8b01657
J. Am. Chem. Soc. XXXX, XXX, XXX–XXX

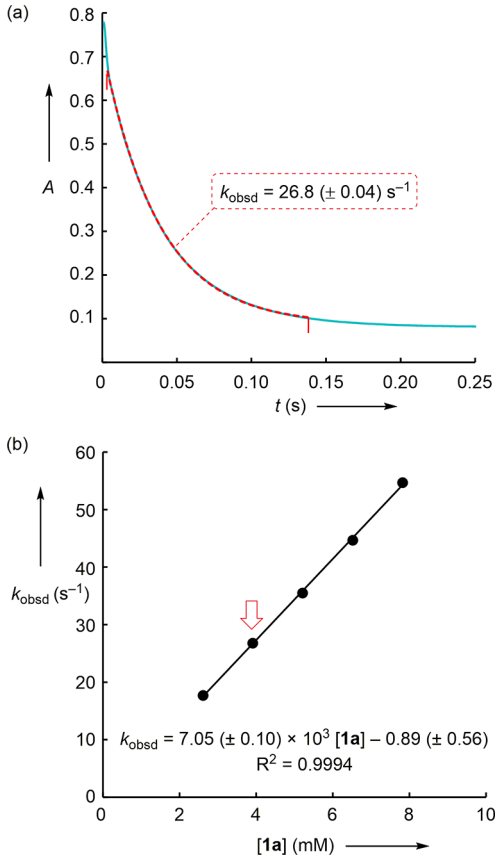

Figure 1. (a) Monoexponential decay of the absorbance A of **2b** (at 405 nm) during the reaction of **1a** (3.91×10^{-3} mol L^{-1}) with **2b** (2.50×10^{-4} mol L^{-1}) in DMSO at 20 °C (the remaining absorbance is due to products generated by degradation of carbanion **2b**). (b) k_{obsd} for the reaction of **1a** with **2b** versus the concentration of **1a**.

1b) correspond to the second-order rate constants k_2^{exptl} listed in Scheme 2.

Table 1 shows the role of counterions on the reaction kinetics. Neither addition of 18-crown-6 ether to the potassium salts of **2a** or **2b** nor exchange of *t*-BuOK by Schwesinger's base P_4-^{t}Bu[18] for the generation of **2b** from its conjugate acid had a significant effect on the second-order rate constants k_2^{exptl}.

Determination of the Rate-Limiting Step. As shown in Scheme 3, nucleophilic attack of **2** at the ketone **1** yields the intermediate alkoxide anion **4**, which either cyclizes with formation of the epoxide **3** or undergoes retroaddition with regeneration of ketone **1** and carbanion **2**.

The time-dependent concentrations of **2**, **4**, and **3** can be expressed by eqs 2–4.

$$d[\mathbf{2}]/dt = -k_{CC}[\mathbf{1}][\mathbf{2}] + k_{-CC}[\mathbf{4}] \quad (2)$$

Scheme 3. Mechanism of the Reactions of Arylsulfonyl-Substituted Chloromethyl Anions with Ketones

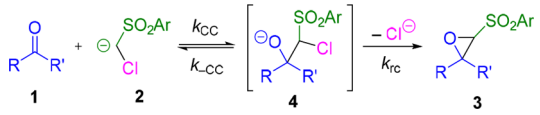

$$d[\mathbf{4}]/dt = k_{CC}[\mathbf{1}][\mathbf{2}] - k_{-CC}[\mathbf{4}] - k_{rc}[\mathbf{4}] \quad (3)$$

$$d[\mathbf{3}]/dt = k_{rc}[\mathbf{4}] \quad (4)$$

As the intermediate β-chloroalkoxide anion **4** is formed as a short-lived species, the Bodenstein approximation holds ($d[\mathbf{4}]/dt = 0$), and the concentration of **4** is given by eq 5. Substitution into eq 4 yields eq 6, and k_2^{exptl} is a function of k_{CC}, k_{-CC}, and k_{rc} as shown by eq 7.

$$[\mathbf{4}] = k_{CC}[\mathbf{1}][\mathbf{2}]/(k_{-CC} + k_{rc}) \quad (5)$$

$$\Rightarrow d[\mathbf{3}]/dt = -d[\mathbf{2}]/dt = k_{CC}k_{rc}[\mathbf{1}][\mathbf{2}]/(k_{-CC} + k_{rc}) \quad (6)$$

$$\Rightarrow k_2^{exptl} = k_{CC}/(k_{-CC}/k_{rc} + 1) \quad (7)$$

According to eq 7, the rate of the attack of **2** at the carbonyl group (k_{CC}) can be derived from the measured rate constant k_2^{exptl} (Scheme 2) if the ratio k_{-CC}/k_{rc} is known. To determine k_{-CC}/k_{rc}, we have developed an independent access to the intermediate **4**.

Synthesis of the Halohydrins 4-H. Whereas treatment of **2**-H with base in the presence of ketones **1** at ambient temperature led to the formation of the epoxides **3** (Scheme 2), the reactions of **2a**-H with BuLi or of **2b**-H with lithium diisopropylamide (LDA) in THF at −78 °C, followed by addition of the ketones **1a–j**, and subsequent acidification at low temperature yielded the halohydrins **4**-H in good yields (Scheme 4).[19] In the case of the acyclic ketones **1i** and **1j**, two diastereomeric compounds were formed, which were separated by column chromatography on silica gel and fully characterized. The structure of **4ca**-H was confirmed by single-crystal X-ray crystallography and showed a conformer with chlorine *gauche* to the hydroxyl group (Figure 2).

Examination of the Reversibility of the Attack of 2 at the Ketones 1. To examine whether the intermediates **4**, generated by treatment of the halohydrins **4**-H with base, undergo ring closure with formation of **3** (k_{rc}, Scheme 3) or retroaddition with regeneration of **1** and **2** (k_{-CC}, Scheme 3), it was necessary to find a trapping reagent which rapidly intercepts **2** after its generation from **4**. In view of their high reaction rates (Scheme 2), ketones **1g**, **1j**, **1k**, and **1l** were considered to be suitable trapping agents. Ketone **1j** was then eliminated from this series because the resulting oxirane **3jb** turned out not to be stable at 20 °C.

Table 1. Second-Order Rate Constants k_2^{exptl} (M^{-1} s^{-1}) for the Reactions of the Ketones 1 with Carbanions 2 under Various Conditions

ketone	nucleophile	k_2^{exptl}, [a]	k_2^{exptl}(18-crown-6)[b]	k_2^{exptl}(P_4-^{t}Bu)
1e	**2a**	$(1.77 \pm 0.13) \times 10^4$	$(1.79 \pm 0.11) \times 10^4$	
1f	**2b**	$(7.62 \pm 0.35) \times 10^3$	$(7.65 \pm 0.47) \times 10^3$	
1g	**2b**	$(1.81 \pm 0.07) \times 10^4$	$(1.71 \pm 0.04) \times 10^4$	$(1.66 \pm 0.05) \times 10^4$
1j	**2b**	$(3.21 \pm 0.55) \times 10^4$	$(3.59 \pm 0.33) \times 10^4$	

[a] Data from Scheme 2. [b] 18-Crown-6 (2.0–2.5 equiv) was added to the potassium salts of **2a**,**b**.

DOI: 10.1021/jacs.8b01657
J. Am. Chem. Soc. XXXX, XXX, XXX–XXX

Scheme 4. Synthesis of the Halohydrins 4-H

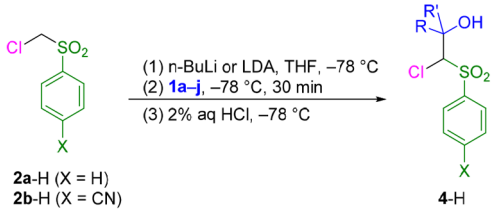

ketone	nucleophile	product (yield)
1a	2b	4ab-H (90%)
1b	2b	4bb-H (85%)
1c	2a	4ca-H (90%)
	2b	4cb-H (85%)
1d	2a	4da-H (85%)
1e	2a	4ea-H (75%)
	2b	4eb-H (95%)
1f	2b	4fb-H (80%)
1g	2b	4gb-H (70%)
1h	2a	4ha-H (70%)
	2b	4hb-H (95%)
1i	2a	4ia-H (93%, dr 1.8/1)
1j	2b	4jb-H (83%, dr 1.1/1)

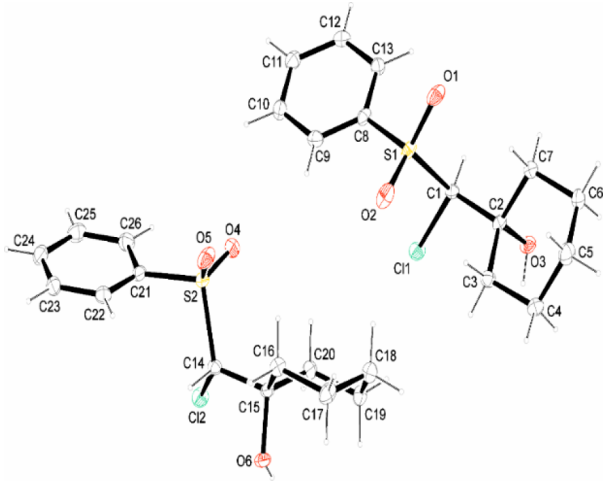

Figure 2. ORTEP drawing of the crystal structure of **4ca**-H (the ellipsoid probability level is 50%).

Scheme 5. Competition Reactions To Examine the Suitability of Ketones 1g,k,l as Trapping Agents

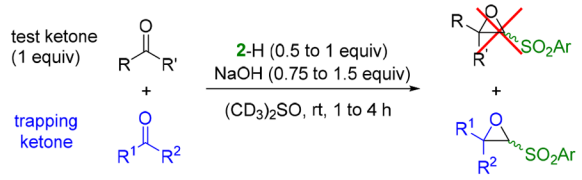

test ketone	trapping ketone	nucleophile	product
1c 1d 1h 1i	1g (1 equiv) 1g (1 equiv) 1g (3 equiv) 1g (1 equiv)	2a 2a 2a 2a	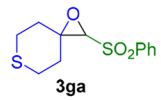 3ga
1a–1d, 1f–1h 1e	1l (3 equiv) 1l (3 equiv)	2b 2a	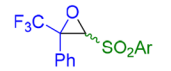 3la or 3lb
1j	1k (7 equiv)	2b	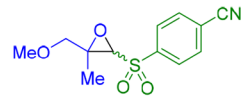 3kb

Scheme 6. Crossover Reaction of the Cyclohexanone Adduct 4ca-H

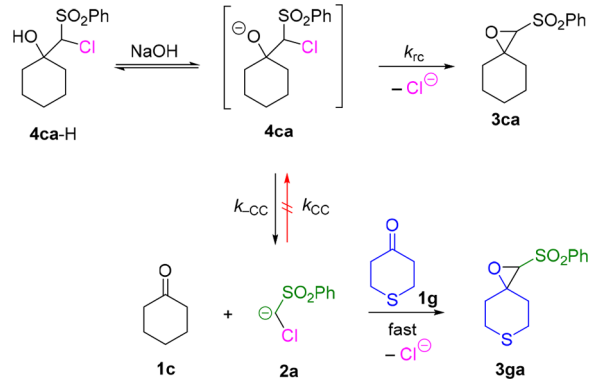

When 1/1 mixtures of **1g** on one side and of **1c**, **1d**, or **1i** on the other were combined with 0.5 equiv of the carbanion **2a**, the oxiranes derived from **1g** (i.e., **3ga**) were formed exclusively (Scheme 5). Since **1g** is only 6 times more reactive than **1h**, 3 equiv of **1g** was employed to obtain **3ga** exclusively from a mixture of **1h** and **1g**.

The oxiranes **3la** and **3lb** were the only products obtained from the reactions of 3/1 mixtures of **1l** and **1a**–**h** with **2** (1 equiv with respect to **1a**–**h**). Since the product obtained by treatment of a mixture of **1j** and **1l** with **2b** was difficult to analyze, **1k** was used as a trapping agent, and treatment of a 7/1 mixture of **1k** and **1j** with 1 equiv of **2b** gave the oxirane **3kb** exclusively.

The principle of the crossover experiments is illustrated in Scheme 6. When the independently synthesized halohydrin **4ca**-H is treated with NaOH in the presence of the highly reactive ketone **1g**, the generated intermediate **4ca** has the choice of undergoing either ring closure with formation of the epoxide **3ca** or retroaddition with regeneration of **1c** and **2a**. As **1g** is considerably more reactive and present in higher concentration than **1c**, any regenerated carbanion **2a** will exclusively be converted into the crossover product **3ga**, and the ratio [**3ga**]/[**3ca**] equals the ratio k_{-CC}/k_{rc}.

Scheme 7 shows that in all crossover experiments at least 3 equiv of trapping agents was employed to ensure that they will quantitatively intercept the regenerated carbanions **2**. In Scheme 7, one can furthermore see that, in most cases investigated, ring closure (k_{rc}) is up to 8 times faster than retroaddition. Entries 5–7 show, however, that the intermediates generated from cycloheptanone (**1d**) undergo retroaddition 3–4 times faster than ring closure. Comparison of entry 5 with entry 7 and of entry 13 with entry 14 indicates that almost the same k_{-CC}/k_{rc} ratio is obtained with different trapping agents, and entries 5/6 and 8/9 show that the nature of the counterion (K^+ vs Na^+) has only a small influence on this ratio. The similarity of k_{-CC}/k_{rc} in entries 3/4, 8/10, and 13/15 implies that the ratio of retroaddition vs ring closure is almost independent of the substituents at the arylsulfonyl groups. Entries 16/17 as well as 18/19 show that the two diastereomeric halohydrins obtained from the asymmetric ketones **1i** and **1j** react with significantly different k_{-CC}/k_{rc} ratios.

DOI: 10.1021/jacs.8b01657
J. Am. Chem. Soc. XXXX, XXX, XXX–XXX

Scheme 7. Crossover Reactions of 4-H

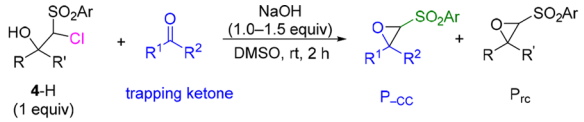

4-H (1 equiv) | trapping ketone | P_{-CC} | P_{rc}

entry	halohydrin	trapping ketone	$P_{-CC}/P_{rc} = k_{-CC}/k_{rc}$[a]
1	**4ab**-H	**1l** (4 equiv)	0.89
2	**4bb**-H	**1l** (4 equiv)	0.63
3	**4ca**-H	**1g** (3 equiv)[b]	0.60
4	**4cb**-H	**1l** (4 equiv)[b]	0.86
5	**4da**-H	**1g** (3 equiv)[b]	3.5
6		**1g** (3 equiv)[c]	3.3
7		**1l** (3 equiv)	4.1
8	**4ea**-H	**1l** (4 equiv)	0.37
9		**1l** (4 equiv)[c]	0.29
10	**4eb**-H	**1l** (4 equiv)	0.33
11	**4fb**-H	**1l** (4 equiv)	0.13
12	**4gb**-H	**1l** (4 equiv)	0.57
13	**4ha**-H	**1g** (4 equiv)	0.19
14		**1l** (4 equiv)	0.24
15	**4hb**-H	**1l** (4 equiv)	0.21
16	**4ia'**-H	**1g** (3 equiv)[b]	2.2
17	**4ia''**-H	**1g** (3 equiv)	6.9
18	**4jb'**-H	**1k** (8 equiv)	2.2
19	**4jb''**-H	**1k** (8 equiv)	5.1

[a]Determined by ^{1}H NMR spectroscopic analysis of the crude product. [b]Product yields determined by using 1,3,5-trimethoxybenzene as an internal standard (Supporting Information). [c]KOH was used as the base instead of NaOH.

Combination of the k_{-CC}/k_{rc} ratios from Scheme 7 with k_2^{exptl} from Scheme 2 according to eq 7 yields the rate constants for nucleophilic attack of **2** at the ketones **1** (k_{CC}), which are listed in Table 2. While this procedure is straightforward for the reactions with symmetrical ketones, the situation is more complex for unsymmetrical ketones because their reactions with the carbanions **2** yield mixtures of diastereomeric halohydrins **4**-H, as specified for **1i** and **1j** in the last two entries of Table 2.

The stereospecifity of ring closure has exemplarily been studied for the reaction of **2a** with pentan-2-one (**1i**). The diastereomeric halohydrins **4ia′**-H and **4ia″**-H undergo either stereospecific ring closure with formation of epoxides or retroaddition with regeneration of **1i** and **2a**. Figure 3a shows the ^{1}H NMR spectrum of **3ga**, the product formed by trapping the regenerated carbanion **2a** with the ketone **1g**. Treatment of ketone **1i** with anion **2a** yielded a mixture of the diastereomeric epoxides **3ia′** and **3ia″** (Figure 3b). Since the ring protons A′ and A″ of the epoxides **3ia′** and **3ia″** have similar chemical shifts, their ratio was derived from the ^{1}H NMR signals of the methyl groups B′/B″ and C′/C″. Nuclear Overhauser effect (NOE) experiments show that the methyl resonances at lower field (B′ and C″) arise from the groups *cis* to the phenylsulfonyl substituent.[20] Parts c and d of Figure 3 reveal that the epoxides **3ia′** and **3ia″** are formed stereospecifically from the diastereomeric halohydrins **4ia′**-H and **4ia″**-H, respectively. When **4ia′**-H is treated with NaOH in the presence of **1g**, epoxides **3ia′** and **3ga** are formed in the ratio 1/2.2, as derived from the integrals of protons A′ and A in Figure 3c. Since there are no peaks at δ 1.32 and 0.93, the chemical shifts of the methyl protons (B″ and C″) of the diastereomer **3ia″**, we can conclude that **4ia′** either cyclizes with formation of **3ia′** or fragments with formation of **1i** and **2a**, the latter of which is subsequently trapped by **1g** to give **3ga**.

Analogously, treatment of the other diastereomer (**4ia″**-H) with NaOH in the presence of **1g** yields the epoxides **3ia″** and **3ga** in a ratio of 1/6.9 (from integrals A″ and A, Figure 3d). The stereospecificity of this cyclization, i.e., the exclusive formation of **3ia″** from **4ia″**-H, can be derived from the absence of **3ia′** in the product mixture, which would be detectable by a ^{1}H NMR signal for the methyl group B′ at δ 1.63 and less clearly by the methyl triplet at δ 0.80 for C′.

With the product ratio **3ia′**/**3ia″** = 2.6 given in Scheme 2, we can split the measured gross second-order rate constant k_2^{exptl} = 74.2 M^{-1} s^{-1} for the reaction of **1i** with **2a** (Scheme 2) into the partial rate constants $k_2'^{(exptl)}$ = 53.6 M^{-1} s^{-1} and $k_2''^{(exptl)}$ = 20.6 M^{-1} s^{-1} for the formation of **3ia′** and **3ia″**, respectively. The ratio of these partial rate constants corresponds to the observed product ratio (eq 8) given in Scheme 2, and their sum corresponds to the measured rate constants (k_2^{exptl} in Scheme 2, eq 9).

$$k_2'^{(exptl)}/k_2''^{(exptl)} = 2.6 \quad (8)$$

$$k_2'^{(exptl)} + k_2''^{(exptl)} = k_2^{exptl} = 74.2\ M^{-1}\ s^{-1} \quad (9)$$

Table 2. Determination of Second-Order Rate Constants k_{CC} from Measured Rate Constants k_2^{exptl} and Ratios k_{-CC}/k_{rc}

ketone	nucleophile	k_2^{exptl},[a] (M^{-1} s^{-1})	$(k_{-CC}/k_{rc}) + 1$[b]	k_{CC} (M^{-1} s^{-1})	E	k^{calcd}/k_{CC}
1a	**2b**	7.05×10^3	1.89	1.33×10^4	−17.5	identical
1b	**2b**	1.31×10^2	1.63	2.14×10^2	−21.0	identical
1c	**2a**	2.98×10^3	1.60	4.77×10^3	−19.9[c]	0.69
	2b	2.61×10^2	1.86	4.85×10^2		1.6
1d	**2a**	8.49×10^1	4.5	3.8×10^2	−22.1	identical
1e	**2a**	1.77×10^4	1.37	2.42×10^4	−18.4[c]	0.58
	2b	1.82×10^3	1.33	2.42×10^3		1.9
1f	**2b**	7.62×10^3	1.13	8.61×10^3	−17.9	identical
1g	**2b**	1.81×10^4	1.57	2.84×10^4	−16.9	identical
1h	**2a**	2.12×10^4	1.19	2.52×10^4	−18.2[c]	0.67
	2b	3.00×10^3	1.21	3.63×10^3		1.6
1i	**2a**	7.42×10^1	3.2[d]	3.3×10^2[e]	−22.3	identical
			7.9[d]			
1j	**2b**	3.21×10^4	3.2[d]	1.3×10^5[e]	−15.6	identical
			6.1[d]			identical

[a]From Scheme 2. [b]From Scheme 7. [c]Calculated by averaging the individual E parameters. [d]Ratios (k_{-CC}/k_{rc}) for the individual halohydrin diastereoisomers. [e]$k_{CC} = k'_{CC} + k''_{CC}$ (see the text for the calculation).

DOI: 10.1021/jacs.8b01657
J. Am. Chem. Soc. XXXX, XXX, XXX−XXX

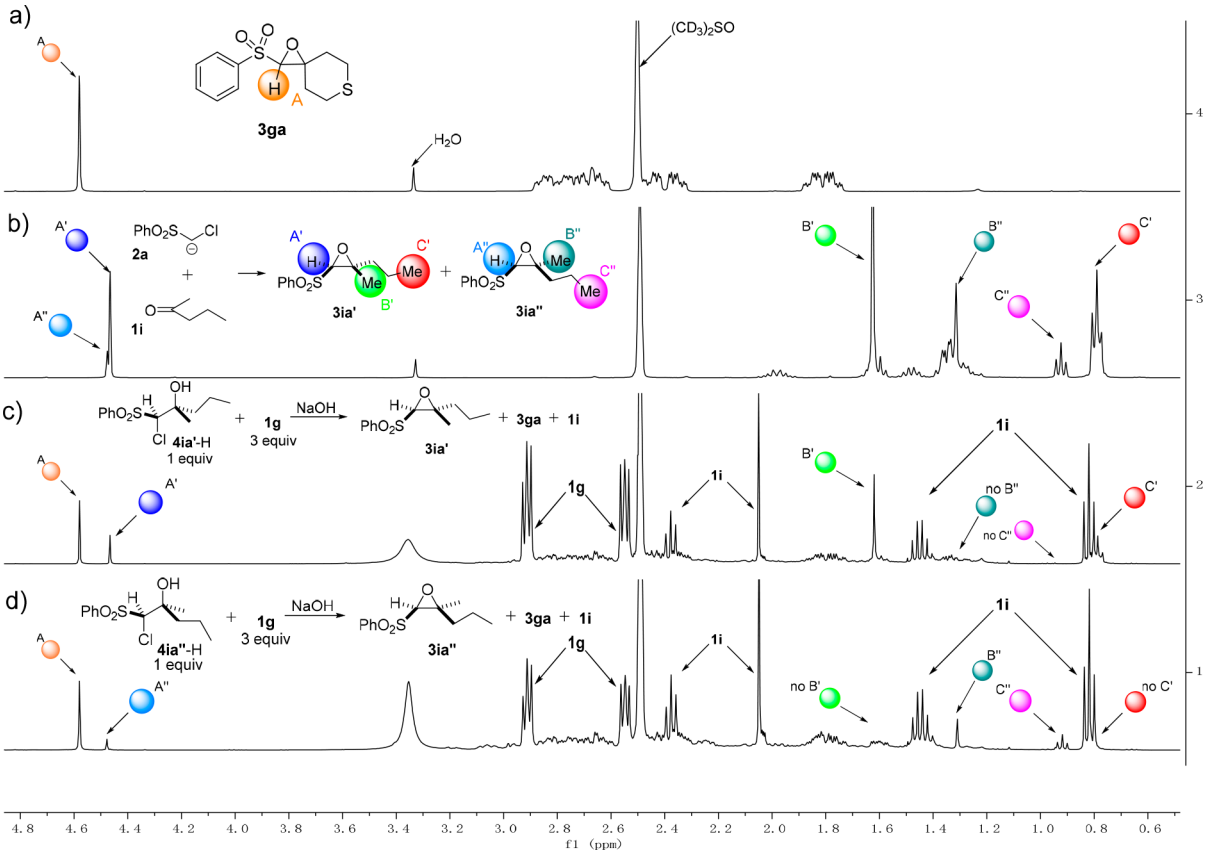

Figure 3. Examination of the stereospecifity of ring closure of the diastereomeric halohydrins **4ia**′-H and **4ia**″-H by ^{1}H NMR spectroscopy: (a) independently synthesized trapping product of regenerated **2a**, (b) mixture of **3ia**′ and **3ia**″ obtained from the reaction of **2a** with **1i**, (c) exclusive formation of **3ia**′ and **3ga** (1/2.2 = k'_{rc}/k'_{-CC}) by treatment of **4ia**′-H with NaOH in the presence of **1g**, (d) exclusive formation of **3ia**″ and **3ga** (1/6.9 = k''_{rc}/k''_{-CC}) by treatment of **4ia**″-H with NaOH in the presence of **1g**.

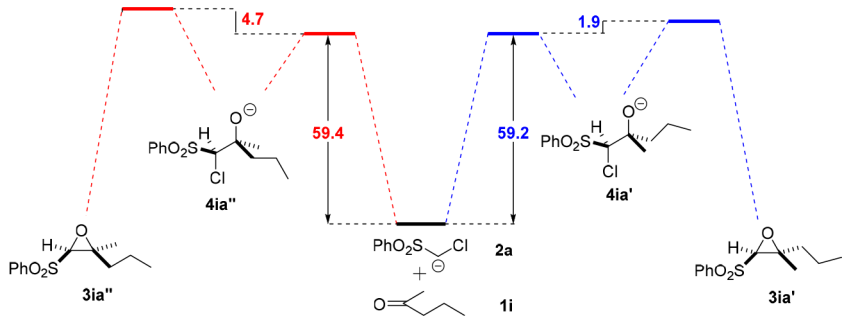

Figure 4. Gibbs energy profile (kJ mol^{-1}) for the reaction of carbanion **2a** with pentan-2-one (**1i**) at 20 °C in DMSO derived from rate measurements (Scheme 2) and crossover experiments (Figure 3, Table 2).

With application of eq 7 to the two parallel reactions with k'_{-CC}/k'_{rc} = 2.2 (Figure 3c and Scheme 7, entry 16) and k''_{-CC}/k''_{rc} = 6.9 (Figure 3d and Scheme 7, entry 17), we obtain k'_{CC} = (2.2 + 1) × 53.6 M^{-1} s^{-1} = 1.7 × 10^2 M^{-1} s^{-1} and k''_{CC} = (6.9 + 1) × 20.6 M^{-1} s^{-1} = 1.6 × 10^2 M^{-1} s^{-1}, i.e., both halohydrins are formed with similar rates, and the stereoselectivity originates from the different rates of cyclization as illustrated in Figure 4. In contrast, in THF at −78 °C, **4ia**′-Li is formed 1.8 times faster than **4ia**″-Li (Scheme 4).

An analogous calculation gave k'_{CC} = 7.1 × 10^4 M^{-1} s^{-1} and k''_{CC} = 6.1 × 10^4 M^{-1} s^{-1} for the reaction of **2b** with the unsymmetrical ketone **1j**.

Substitution of k_{CC} and the published parameters N and s_N for **2a**,**b** into eq 1 yielded the electrophilicity parameters E of the ketones **1**. In cases where the electrophilicity parameters E are derived from reactions with **2a** and **2b**, both rate constants should ideally give the same value of E. As this is not the case, the E values derived from different reactions were averaged and listed in Table 2. The last column of Table 2, which compares the rate constants calculated by eq 1 with the directly determined rate constants, shows that, in this series, eq 1 reproduces the rate constants k_{CC} within a factor of 2.

A confirmation for the ketone reactivities derived in this way was obtained by competition experiments. When a mixture of diethyl maleate (**5**) (E = −19.49) and cycloalkanone **1b** or **1c** was treated with **2a** (in situ generated from **2a**-H and NaOH), mixtures of the epoxides **3** and the cyclopropane **6** were obtained. Their ratio was determined by ^{1}H NMR spectroscopy

DOI: 10.1021/jacs.8b01657
J. Am. Chem. Soc. XXXX, XXX, XXX−XXX

and used to calculate the ratio $k_2^{exptl}(\mathbf{1})/k_2^{exptl}(\mathbf{5})$ given in Scheme 8. The ratios of direct rate measurements, $k_2(\mathbf{1})/k_2(\mathbf{5})$,

Scheme 8. Examination of the *E* Parameters of Ketones 1

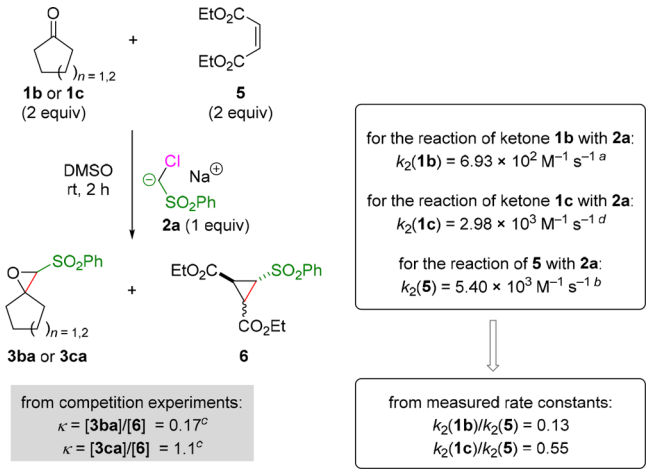

[a]Equation 1 gives $k_{CC} = 1.13 \times 10^3$ M^{-1} s^{-1}, which was corrected for reversibility by applying eq 7 with $k_{-CC}/k_{rc} = 0.63$. [b]This work (Table S20, Supporting Information). [c]For the calculation, see the Supporting Information. [d]From Scheme 2.

agree with product ratios from competition experiments, κ = [**3**]/[**6**], within a factor of 2. This suggests that diethyl maleate (**5**) and cyclohexanone (**1c**) have similar electrophilicities *E*, one order of magnitude greater than the electrophilic reactivity of cyclopentanone (**1b**).

Intrinsic Reaction Pathway Calculations. The mechanistic picture derived from the kinetic studies was subsequently complemented by reaction path calculations. Geometry optimizations and calculations of intrinsic reaction pathways have been performed at the B3LYP[21]-D3[22]/6-31+G(d,p)[23] level of theory in combination with the polarizable continuum model (PCM)[24] for DMSO as the solvent and UA0 radii. Improved energies for ground and transition states have been calculated at the PCM(DMSO,UA0)/B2PLYP[25]-D3/def2TZVPP[26] level. Combination of energies with thermochemical corrections obtained at a lower level then yields the reaction Gibbs energies reported in the Supporting Information and summarized in Figures 5–7.

For the reaction of carbanion **2a** with cyclohexanone (**1c**) (a ketone of intermediate electrophilicity, $E = -19.9$), the Gibbs energy surface is shown in Figure 5. Two distinct pathways have been identified for the addition of anion **2a** to the C=O double bond in ketone **1c**, which differ by the relative orientation of the two reactants. The energies shown are those of the energetically best conformers for each pathway (for full details, see the Supporting Information). The blue, energetically less favorable reaction pathway ($\Delta G^{\ddagger}$ = +61.5 kJ mol^{-1}) directly yields an adduct with the C–Cl bond *anti* to the C–O bond. Chloride expulsion through epoxide ring closure is possible from this adduct with a barrier of +44.8 kJ mol^{-1} (relative to separate reactants). A second, red reaction pathway ($\Delta G^{\ddagger}$ = +47.4 kJ mol^{-1}) leads to a primary adduct where the C–Cl bond assumes a *gauche* orientation relative to the C–O bond. Epoxide ring closure from this adduct is not immediately possible, but requires rotation around the newly formed C–C bond such that the C–Cl and C–O bonds attain the *anti* orientation required for cyclization. The barrier for this

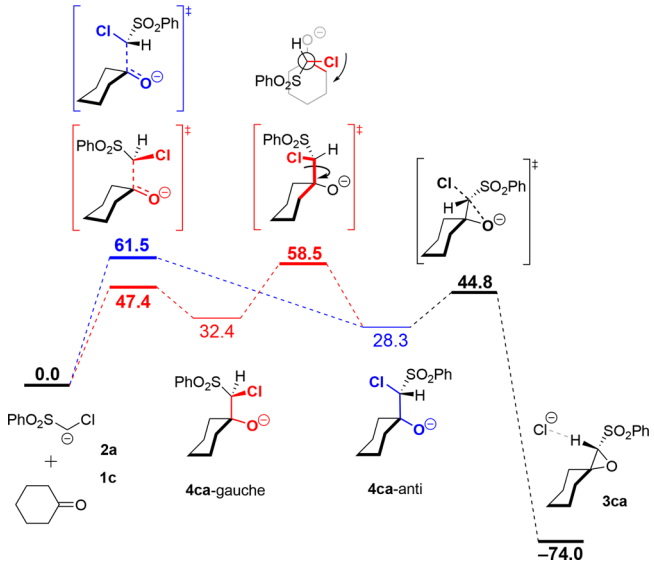

Figure 5. Gibbs energy surface (25 °C) for the reaction of **1c** with **2a** [at the PCM(DMSO,UA0)/B2PLYP-D3/def2TZVPP//PCM-(DMSO,UA0)/B3LYP-D3/6-31+G(d,p) level, kJ mol^{-1}].

rotation is higher ($\Delta G^{\ddagger}$ = +58.5 kJ mol^{-1} relative to separate reactants) than the barrier for the reversal to the separate reactants **2a** and **1c**. The comparable heights of the barriers for initial nucleophilic addition and conformational reorientation are in line with the results derived from the crossover experiments with halohydrin **4ca**-H described in Scheme 7. Guided by the conformational analysis of halohydrin **4ca**-H and its deprotonated form **4ca**, we assume that **4ca**-H exists as a mixture of conformers in solution, from which only that with the C–Cl and C–O bonds in *gauche* conformation had crystallized (see Figure 2 and Figure S15 in the Supporting Information). Deprotonation of **4ca**-H will give both adduct conformers shown in Figure 5. While the adduct **4ca** with *gauche* C–Cl and C–O bonds will revert back to reactants, the conformer with *anti* C–Cl/C–O orientation will cyclize to epoxide **3ca**.

The reaction of anion **2a** with the more reactive ketone **1g** (E = −16.9) has been studied analogously. The resulting Gibbs energy surface in Figure 6 shows that the nucleophilic addition can also lead to intermediates **4ga** with C–Cl/C–O *gauche* or *anti* orientation, and the rotational barrier for their interconversion ($\Delta G^{\ddagger}$ = +41.4 kJ mol^{-1} relative to separate reactants) is again comparable to the barriers of the reverse reaction. The barrier for epoxide ring closure is, in comparison, lower at $\Delta G^{\ddagger}$ = +30.0 kJ mol^{-1}, which again implies that adducts with C–Cl/C–O *anti* orientation will move forward to epoxide product rather than revert to separate reactants. In agreement with the larger E value of ketone **1g** as compared to **1c** (−16.9 vs −19.9), the calculated overall Gibbs energy barrier for reaction with anion **2a** is much lower for **1g** than for **1c** (+41.6 vs +58.5 kJ mol^{-1}).

To test whether the mechanistic picture obtained for the ketone addition reaction is comparable to that for addition to electron-poor alkenes (Michael acceptors), the reaction of anion **2a** with dimethyl maleate (**5***), as a model for the experimentally studied diethyl maleate (**5**), was also treated computationally (Figure 7). While the same sequence of initial nucleophilic addition, *gauche*/*anti* reorientation, and ring closure was also found for this system, the relative barriers

DOI: 10.1021/jacs.8b01657
J. Am. Chem. Soc. XXXX, XXX, XXX−XXX

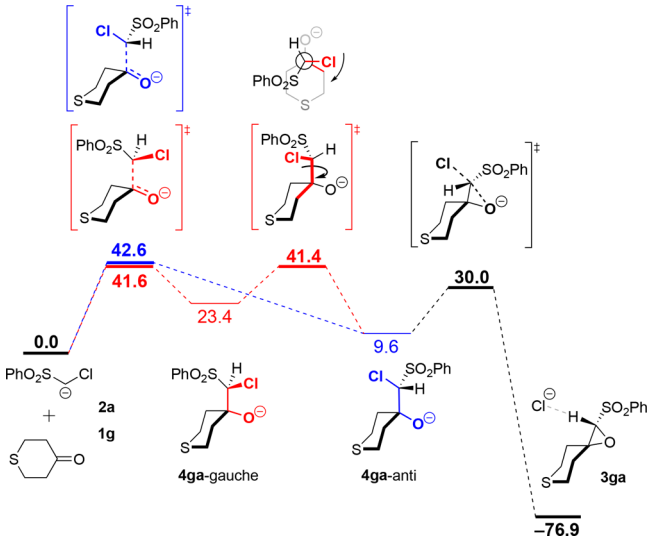

Figure 6. Gibbs energy surface (25 °C) for the reaction of **1g** with **2a** [at the PCM(DMSO,UA0)/B2PLYP-D3/def2TZVPP//PCM-(DMSO,UA0)/B3LYP-D3/6-31+G(d,p) level, kJ mol^{-1}].

for the individual steps differ significantly from those found for the ketones: While the barrier for the initial addition step ($\Delta G^{\ddagger}$ = +46.2 kJ mol^{-1}) is similar to that for ketone **1c** (in line with the kinetic measurements described above), the barriers for rotation and cyclopropane ring closure are much lower than the barrier for the reverse reaction. This implies that the initial addition step of anion **2a** to alkene **5*** is practically irreversible, irrespective of the *gauche*/*anti* orientation in the initial addition step.

Electrophilicities of Benzaldehydes. According to Table 2, most of the ketones characterized in this work have *E* parameters similar to that previously reported for benzaldehyde (**1m**; *E* = −19.5),[2] in contrast to common experience that aldehydes are generally more electrophilic than ordinary ketones. How can this discrepancy be explained?

On the basis of Aggarwal's report that the independently synthesized *anti*-betaine **8a**, formed from sulfonium ylide **7a** and benzaldehyde (**1m**), does not undergo retroaddition but rapidly cyclizes with formation of *trans*-stilbene oxide (**9a**) (Scheme 9),[3c] we had extrapolated that the same was true for the betaine generated from benzaldehyde (**1m**) and *p*-cyano-substituted sulfonium ylide **7b**.[2]

Scheme 9. Aggarwal's Mechanism Accounting for the High *trans* Selectivity in the Epoxidation Reaction of Benzaldehyde with Semistabilized Sulfur Ylide 7a

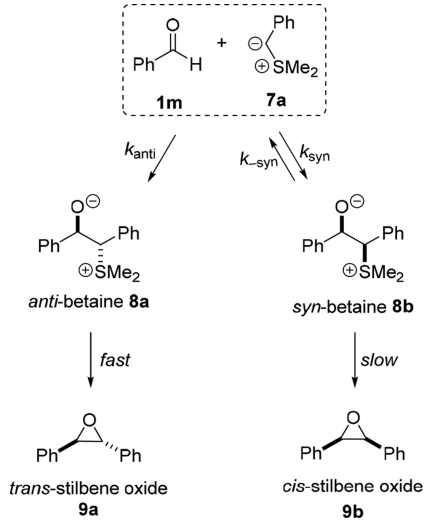

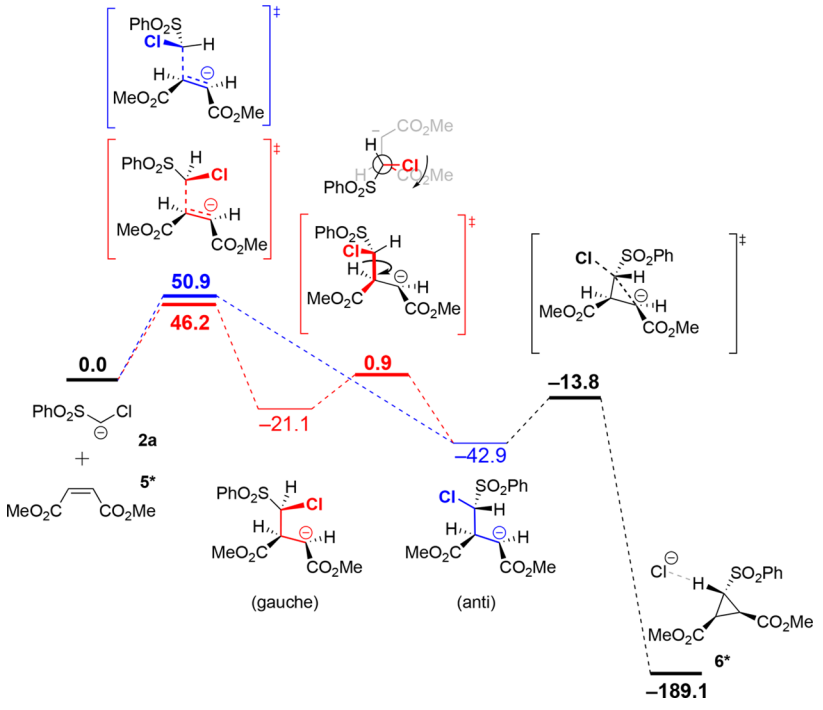

Figure 7. Gibbs energy surface (25 °C) for the reaction of **5*** with **2a** [at the PCM(DMSO,UA0)/B2PLYP-D3/def2TZVPP//PCM(DMSO,UA0)/B3LYP-D3/6-31+G(d,p) level, kJ mol^{-1}]. Dimethyl maleate (**5***) is used as a model substrate for diethyl maleate (**5**).

DOI: 10.1021/jacs.8b01657
J. Am. Chem. Soc. XXXX, XXX, XXX−XXX

This conclusion was obviously incorrect as shown by the following experiments. Treatment of the benzyl thioether **10** with LDA and benzaldehyde (**1m**) yielded the *β*-thio-substituted alcohol **11**, which was converted into the sulfonium tetrafluoroborate **12** by treatment with trimethyloxonium tetrafluoroborate (Scheme 10a). As shown in Scheme 10b,

Scheme 10. Synthesis of Sulfonium Tetrafluoroborate 12 and Crossover Experiment To Elucidate the Rate-Determining Step in the Epoxidation of Benzaldehyde with the Sulfonium Ylide 7b

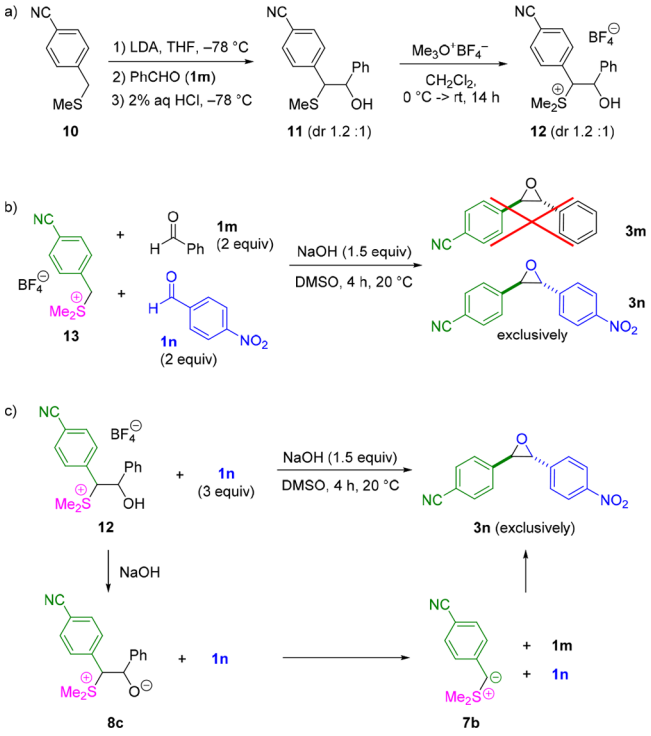

the sulfonium ylide generated by treatment of the sulfonium ion **13** with NaOH in the presence of *p*-nitrobenzaldehyde (**1n**) and benzaldehyde (**1m**) reacts exclusively with the former to yield the epoxide **3n**. As expected, *p*-nitrobenzaldehyde (**1n**) is much more reactive than the parent benzaldehyde (**1m**).

The crossover experiment in Scheme 10c shows the exclusive formation of the epoxide **3n** when **12** is treated with base in the presence of *p*-nitrobenzaldehyde (**1n**). This observation implies that the betaine **8c**, which is formed by deprotonation of **12**, does not cyclize, but rather undergoes retroaddition with regeneration of benzaldehyde (**1m**) and the sulfonium ylide **7b**, which is quantitatively intercepted by *p*-nitrobenzaldehyde (**1n**). The rate-determining step for the reaction of the sulfonium ylide **7b** with benzaldehyde (**1m**) thus is the cyclization and not the nucleophilic attack of the ylide at the carbonyl group, as assumed for the derivation of the electrophilic reactivity of benzaldehyde (**1m**) in ref 2. The electrophilicity parameters of aldehydes reported in ref 2 thus do not refer to the initial attack of nucleophiles at the carbonyl group but describe the gross rate constants for the reactions of carbonyl groups with the sulfonium ylide **7b**.

How can the rate of the initial nucleophilic attack at aldehydes be determined? Are the chloro-substituted carbanions **2a**,**b** suitable reference nucleophiles, because the corresponding intermediates cyclize with lower barriers than the intermediates formed from sulfur ylides? In line with the expected higher electrophilic reactivity of benzaldehyde (**1m**), its reactions with the carbanions **2a**,**b** were found to be too fast for direct measurements with our stopped-flow techniques. We succeeded, however, to measure the rate of the reaction of **2b** with the less electrophilic *p*-methoxybenzaldehyde (**1o**) in the same way as described above for the corresponding reactions with ketones and obtained the second-order rate constant k_2^{exptl} = 2.69 × 10^4 M^{-1} s^{-1}, which will be used in Table 3. Subsequently, the relative reactivities of benzaldehyde (**1m**) and *p*-methoxybenzaldehyde (**1o**) toward **2a** were determined by the competition experiment illustrated in Scheme 11.[27]

Scheme 11. Competition Experiments for Determining the Relative Reactivities of Benzaldehyde (1m) and *p*-Methoxybenzaldehyde (1o) toward 2a

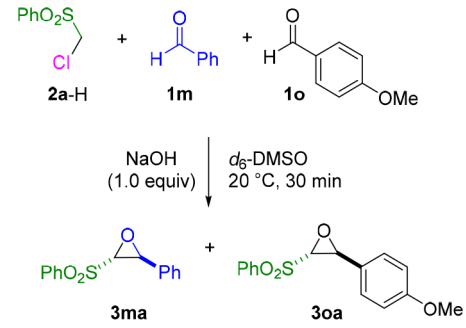

[2a-H]/[1m]/[1o]	[3ma]/[1m]	[3oa]/[1o]	κ
1 / 2 / 2	0.86/2.55	0.08/3.60	13
1 / 2 / 5	0.78/2.51	0.20/8.49	12

From the composition of the reaction mixtures given in Scheme 11, we derived the competition constant *κ* using eq 10,[28] which is applicable when the competing reagents are not used in high excess and the ratio of their concentrations changes during the reaction.

$$\kappa = \frac{k_2^{exptl}(\mathbf{1m})}{k_2^{exptl}(\mathbf{1o})} = \frac{\log\left(\frac{[\mathbf{1m}]_o}{[\mathbf{1m}]_t}\right)}{\log\left(\frac{[\mathbf{1o}]_o}{[\mathbf{1o}]_t}\right)} = \frac{\log\left(1 + \frac{[\mathbf{3ma}]_t}{[\mathbf{1m}]_t}\right)}{\log\left(1 + \frac{[\mathbf{3oa}]_t}{[\mathbf{1o}]_t}\right)} \quad (10)$$

From the directly measured rate constant for the reaction of **2b** with **1o** and the competition constant *κ* (Scheme 11), one can calculate the rate constant k_2^{exptl} for the reaction of **2b** with benzaldehyde (**1m**) according to eq 11.

$$k_2^{exptl}(\mathbf{1m}) = \kappa k_2^{exptl}(\mathbf{1o}) \quad (11)$$

As described in Scheme 3 and eqs 2–7, the rate constants k_2^{exptl} thus obtained refer to the rates of the overall reactions. To derive the rate of attack of the anions **2** at the carbonyl groups of the aldehydes **1m** and **1o** (k_{CC}), we must know the degree of reversibility of the initial addition step, which again was determined by crossover experiments. For their design, it was necessary to identify trapping agents which can quantitatively intercept the carbanions **2** generated by reverse addition of the halohydrin anions. As shown in Scheme 12, the epoxides **3la′** and **3la″** are formed exclusively when a 1/1 mixture of benzaldehyde (**1m**) and trifluoroacetophenone (**1l**) is treated with 0.5 equiv of **2a**, indicating that the fluorinated ketone **1l** is much more electrophilic than benzaldehyde (**1m**).

DOI: 10.1021/jacs.8b01657
J. Am. Chem. Soc. XXXX, XXX, XXX–XXX

Scheme 12. Competition Experiment To Demonstrate the Much Higher Reactivity of Ketone 1l Compared to Benzaldehyde (1m)

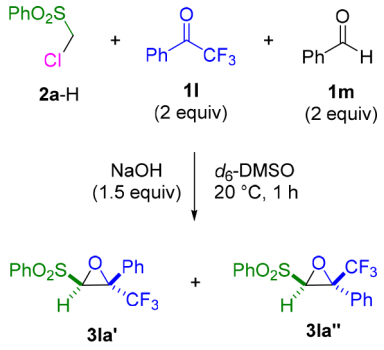

In analogy to the procedure described in Scheme 4, the chlorohydrins **4ma**-H and **4oa**-H (Scheme 13) were synthesized in THF at −78 °C by the reaction of **2a**-Li with the aldehydes **1m** and **1o**, respectively, and subsequent acidification. As illustrated in Scheme 13, treatment of a 1/5 mixture of **4ma**-H and **1l** gave the crossover product **3la** in addition to **3ma**, the cyclization product of **4ma**, in a ratio of 7.9/1. Since **1l** is much more electrophilic than **1m** (Scheme 12), we can conclude that **3ma** is exclusively formed by direct cyclization of the deprotonated chlorohydrin **4ma**, whereas the carbanion **2a**, which is formed by reversal of **4ma**, is quantitatively converted into **3la**. The ratio [**3la**]/[**3ma**] = 7.9 (Scheme 13a) thus reflects the ratio k_{-CC}/k_{rc} given in Table 3.

Scheme 13. Crossover Reactions of Aldehydes 1m and 1o

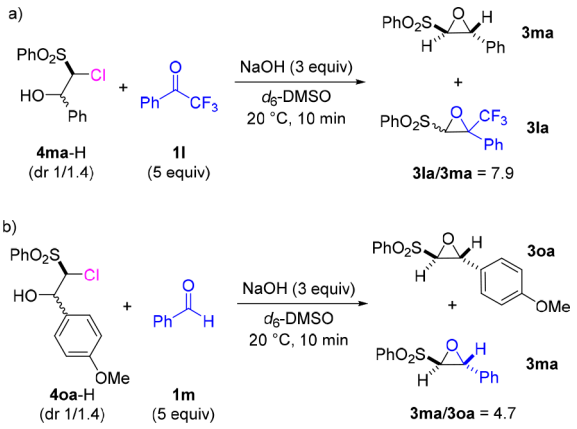

Since the competition experiment in Scheme 11 showed **1m** to be 12 times more reactive than **1o**, benzaldehyde (**1m**) could be used as a trapping reagent for the crossover experiment in Scheme 13b, and the ratio [**3ma**]/[**3oa**] = 4.7 (Scheme 13b) again reflects the ratio k_{-CC}/k_{rc} given in Table 3.

Equation 7 was then used to calculate the rate constants k_{CC} for the nucleophilic attack of **2b** at the aldehydes **1o**,**m** from the gross rate constants k_2^{exptl} listed in Table 3 and the k_{-CC}/k_{rc} ratios from Scheme 13. Substitution into eq 1 with the N and s_N parameters of **2b** eventually yielded the electrophilicity parameters E of the aldehydes **1m** and **1o** in the last column of Table 3. It should be admitted, however, that there are two uncertainties in this derivation. First, the mixtures of diastereomers of the chlorohydrins **4ma**-H and **4oa**-H, which are used for the crossover experiments in Scheme 13, are formed by the reactions with the lithiated nucleophiles **2a**-Li in THF at −78 °C and may differ somewhat from the diastereomeric ratios of the halohydrins generated under the conditions of the kinetic experiments. Second, we had to use the k_{-CC}/k_{rc} ratios for the adducts of **2a** for the calculation of k_{CC} in Table 3 because the epoxides obtained from **2b** were not stable. The plausibility of this assumption is based on the comparison of entries 3/4, 8/10, and 13/15 in Scheme 7, which indicated that the ratio of retroaddition vs ring closure (k_{-CC}/k_{rc}) is almost independent of the substituents at the arylsulfonyl groups.

These uncertainties prompted us to examine the E value for benzaldehyde thus derived by an independent experiment. Substitution of the E values for **1m** and **14** and of the N and s_N parameters for **2a** into eq 1 gives k_{CC}, the rate constant for the initial nucleophilic attack of **2a** at these electrophiles. Since the attack of **2a** at **1m** (in contrast to the attack at **14**) is reversible, k_{CC} was corrected by the splitting ratio k_{-CC}/k_{rc} according to eq 7 to obtain the overall rate constant k_2^{exptl} for the formation of the epoxide **3ma**.

In the competition experiment described in Scheme 14, which compares the electrophilic reactivity of benzaldehyde (**1m**) with that of the *N*-tosyl imine **14**, we observed the ratios [**3ma**]/[**1m**] = 0.22/3.31 and [**15**]/[**14**] = 1.08/2.04 from which the reactivity ratio $\kappa = k(\mathbf{14})/k(\mathbf{1m}) = 6.6$ was derived by

Scheme 14. Competition Experiment To Determine the Relative Reactivities of Benzaldehyde (1m) and Imine 14

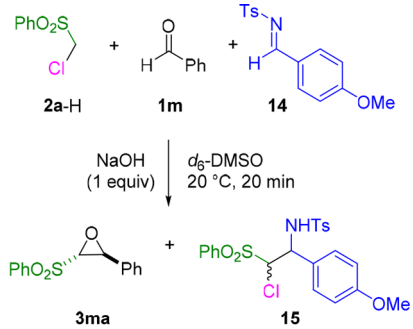

[2a-H]/[1m]/[14]	[3ma]/[1m]	[15]/[14]	κ
1 / 2 / 2	0.22/3.31	1.08/2.04	6.6

Table 3. Derivation of the Rate Constants k_{CC} for Nucleophilic Attack of 2b at the Aldehydes 1o and 1m and the Resulting E Parameters

aldehyde	nucleophile	k_2^{exptl} (M^{-1} s^{-1})	k_{-cc}/k_{rc} [a]	k_{CC} [b] (M^{-1} s^{-1})	approximate E
1m	**2b**	3.36×10^5 [c]	7.9	3.0×10^6	−12.9
1o	**2b**	2.69×10^4 [d]	4.7	1.5×10^5	−15.4

[a]From Scheme 13. [b]From eq 7. [c]From eq 11 using the averaged κ from Scheme 11, $k_2^{exptl} = 12.5 \times (2.69 \times 10^4\ M^{-1}\ s^{-1})$. [d]Direct rate measurement.

DOI: 10.1021/jacs.8b01657
J. Am. Chem. Soc. XXXX, XXX, XXX−XXX

Table 4. Comparison of the Relative Reactivities of Benzaldehyde (1m) and Imine 14 toward 2a Derived from Rate Measurements and Competition Studies

electrophile	E	k_{CC}[a] (M^{-1} s^{-1})	k_2^{exptl} (M^{-1} s^{-1})	k_{rel}(rates)	k_{rel}(competition)
1m	−12.9	2.85×10^6	3.20×10^5[b]	1	1
14	−13.05[c]	2.47×10^6	2.47×10^6	7.7	6.6[d]

[a]From eq 1 with E from this table and N = 28.27 and s_N = 0.42 for **2a**. [b]Calculated with eq 7 using k_{-CC}/k_{rc} = 7.9 from Table 3. [c]Reference 2. [d]From Scheme 14; for a competition experiment with [**2a**-H]/[**1m**]/[**14**] = 1/5/2, a κ = 6.65 was obtained (see the Supporting Information).

Table 5. Quantum Chemically Calculated Frontier Orbital Energies (hartrees), Global (ω) and Local (ω_C) Parr Electrophilicity Indices (eV), and Methyl Anion Affinities (MAAs; kJ mol^{-1}) of Ketones and Aldehydes

electrophile	E[a]	ε_{HOMO}[b]	ε_{LUMO}[b]	global ω[b]	local ω_C[b]	ΔG_{gas}(−MAA)[c]	$\Delta G_{sol\text{-}sp}$(−MAA)[d]
1a	−17.5	−0.24245	−0.02117	1.07	0.16	−131.6	−8.0
1b	−21.0	−0.23597	−0.01449	0.96	0.15	−114.2	14.6
1c	−19.9	−0.23443	−0.01201	0.93	0.15	−126.7	11.7
1d	−22.1	−0.23483	−0.01104	0.92	0.14	−116.3	26.8
1e	−18.4	−0.22444	−0.01456	0.93	0.15	−136.2	2.9
1f	−17.9	−0.24378	−0.02071	1.07	0.18	−147.3	−1.4
1g	−16.9	−0.23250	−0.02310	1.06	0.19	−158.3	−4.1
1h	−18.2	−0.23481	−0.01233	0.93	0.15	−138.5	5.3
1i	−22.3	−0.24272	−0.00948	0.93	0.15	−114.3	16.4
1j	−15.6	−0.22563	−0.02762	1.10	0.14	−144.4	−5.9
1m	(−12.9)[e]	−0.25521	−0.06342	1.80	0.22	−155.2	−27.8
1o	(−15.4)[e]	−0.23442	−0.05149	1.52	0.18	−143.7	−13.2

[a]Empirical electrophilicity parameters from Tables 2 and 3, as defined in eq 1. [b]Calculated at the B3LYP/6-31G(d,p) level in the gas phase. [c]Calculated at the B3LYP/6-311+G(3df,2pd)[32]//B3LYP/6-31G(d,p) level in the gas phase. [d]Based on methyl anion affinities (ΔG_{gas}), which were corrected for solvent effects by adding single-point solvation energies calculated at B3LYP/6-31G(d,p) using the solvation model based on density (SMD)[33] (solvent = DMSO) on gas-phase optimized geometries at the same level. [e]Approximate electrophilicities E of aldehydes (see text and Table 3).

eq 10 as summarized in Table 4. The fair agreement between the relative reactivities of **1m** and **14** and the rate constants calculated by eq 1 confirms the electrophilicity parameter of benzaldehyde (**1m**) derived above.

Correlation Analysis. To elucidate the origin of the corresponding electrophilic reactivities, we have determined various properties of the investigated carbonyl compounds by quantum chemical calculations (Table 5). As specified in Table 5 and Table S25 (Supporting Information), the computational methods used in these calculations differ from those employed in the reaction path calculations (see above) to make them strictly comparable to our earlier work on nucleophilic additions to Michael acceptors and carbenium ions.[29]

Methyl anion affinities (MAAs) have been calculated as the negative of the reaction Gibbs energies for the addition of methyl anion to ketones and aldehydes (eq 12). In addition, we

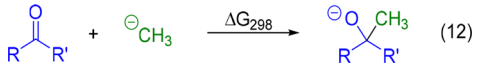

(12)

calculated Parr electrophilicity indices ω (eq 13) for 12 carbonyl compounds[30] from the chemical hardness η (eq 14) and the electronic chemical potential μ (eq 15). The values of η and μ have been calculated from the energies of the lowest unoccupied molecular orbital (ε_{LUMO}) and the highest occupied molecular orbital (ε_{HOMO}), which were derived at the gas-phase B3LYP/6-31G(d,p) level. As in previous studies, the Parr electrophilicity indices are expressed in electronvolts (eV).

$$\omega = \mu^2/2\eta \quad (13)$$

$$\eta = \varepsilon_{LUMO} - \varepsilon_{HOMO} \quad (14)$$

$$\mu = 1/2(\varepsilon_{LUMO} + \varepsilon_{HOMO}) \quad (15)$$

$$\omega_c = \omega f_k^+ \quad (16)$$

The local electrophilicity indices ω_c at the carbonyl carbon were calculated as the product of Parr's electrophilicity index ω and the nucleophilic Fukui function (f_k^+) according to eq 16. The Fukui function for nucleophilic attack is defined as the change of the partial charge q at a certain atom k by adding an electron to the corresponding compound; that is, $f_k^+ = q(k,N+1) - q(k,N)$ with N = total number of electrons.[31]

Previously, good correlations between the electrophilicities of benzhydrylium ions and their LUMO energies were reported by Liu[34a] and Yu.[34b] Figure 8 shows a moderate correlation between the electrophilicity parameters E of ketones and their LUMO energies in the gas phase. This correlation improves slightly when the correlation with LUMO energies in DMSO solution is considered (as depicted in Figure S29B, Supporting Information). Though the correlation between the electrophilicity parameters E and LUMO energies of Michael acceptors has been reported to be very poor,[29a] Figure 8 shows that ketones are generally more electrophilic than Michael acceptors of equal LUMO energies.

Whereas Figure 9 shows a moderate correlation between electrophilicities E and Parr's global electrophilicity index ω, a plot of E vs the local electrophilicity index ω_C (Figure S33A, Supporting Information) has a correlation coefficient of R^2 = 0.30 (!); i.e., ω_C is inadequate to predict electrophilic reactivities of ketones.[35]

As in our previous investigation of the electrophilic reactivities of Michael acceptors,[29a] the electrophilicities E of the ketones **1a**−**1j** correlate fairly with the calculated gas-phase methyl anion affinities (R^2 = 0.77; Figure S17B, Supporting

DOI: 10.1021/jacs.8b01657
J. Am. Chem. Soc. XXXX, XXX, XXX−XXX

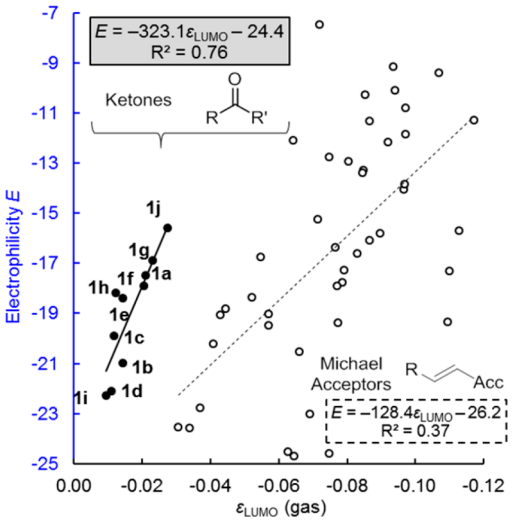

Figure 8. Correlation of the electrophilicities (E) of ketones with their gas-phase lowest unoccupied molecular orbital energies (ε_{LUMO}) calculated at the B3LYP/6-31G(d,p) level of theory compared with the corresponding correlation for Michael acceptors.

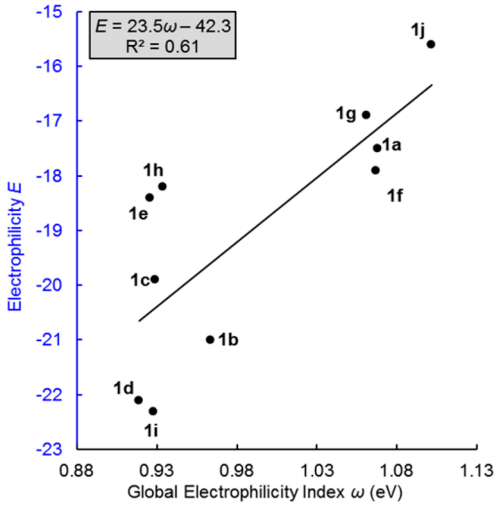

Figure 9. Correlation between electrophilicities (E) of ketones **1a**−**1j** and Parr's global electrophilicity index (ω) calculated at the B3LYP/6-31G(d,p) level of theory.

Information),[21,23,32,36] and this correlation improves further when solvation is included in the calculated methyl anion affinities (Figure 10). Obviously, the solvation energy of the methyl anion is overestimated by this model, since negative MAAs were calculated for several additions. Though the data for the benzaldehydes **1m** and **1o** were not used for the correlation because of the uncertainty of the experimental E parameters, they also are on this best fit line, thus justifying the approximations made for the derivation of their E parameters.

When the plots of E vs MAA for carbonyl compounds and Michael acceptors are drawn in the same graph (Figure 11), one can clearly see two correlation lines, which differ in two aspects. First, the slope for the ketones is significantly larger than that for Michael acceptors. As pointed out previously, the slope of the Michael acceptor correlation implies that in reactions with a nucleophile of $s_N = 0.7$ (see eq 1) about 43% of the differences of the Gibbs reaction energies are reflected in the Gibbs activation energies.[29a] A significantly higher

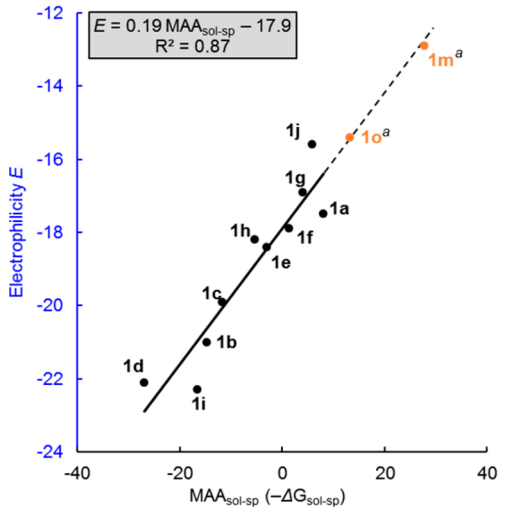

Figure 10. Correlation between electrophilicities (E) of ketones and their $MAA_{sol\text{-}sp}$ values ($-\Delta G_{sol\text{-}sp}$, kJ mol^{-1}) calculated at the SMD(DMSO)/B3LYP/6-311++G(3df,2pd)//B3LYP/6-31G(d,p) level of theory. A superscript *a* indicates the data point was not used for the construction of the correlation line.

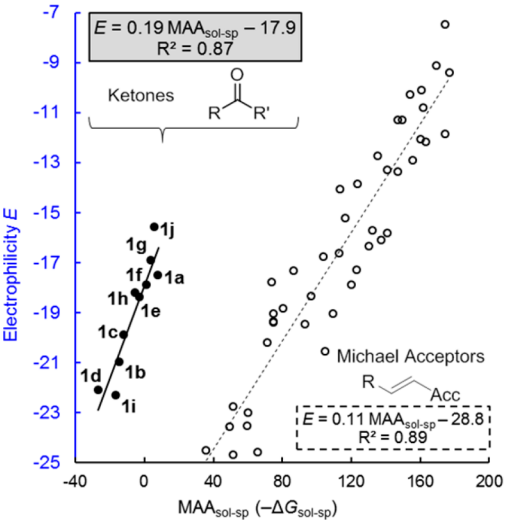

Figure 11. Correlation between the empirical electrophilicities (E, eq 1) and MAA ($-\Delta G_{sol\text{-}sp}$, kJ mol^{-1}) values calculated at the SMD(DMSO)/B3LYP/6-311++G(3df,2pd)//B3LYP/6-31G(d,p) level of theory for ketones and Michael acceptors.

percentage (75%) of the Gibbs reaction energies is mirrored by the activation energies of the additions of nucleophiles with the typical value $s_N = 0.7$ to carbonyl compounds.[37] Second, the different positions of the two correlation lines imply that additions to carbonyl compounds are significantly faster than Michael additions of equal thermodynamic driving force ($\Delta_r G°$). In Marcus terminology,[38a−e] this means that Michael additions proceed with significantly higher reorganization energies than nucleophilic additions to carbonyl groups, which can be explained by the much greater movements of electrons and structural changes occurring in Michael additions (Scheme 15).[38f]

Structure−Reactivity Relationships. As shown in Table 6, the reactivity order cyclobutanone (**1a**) > cyclohexanone (**1c**) > cyclopentanone (**1b**) > cycloheptanone (**1d**), which we found for reactions with carbanions **2a**,**b**, had previously been

DOI: 10.1021/jacs.8b01657
J. Am. Chem. Soc. XXXX, XXX, XXX−XXX

Scheme 15. Less Movement of Electrons and Nuclei Required in Nucleophilic Additions to Carbonyl Groups Than to Michael Acceptors

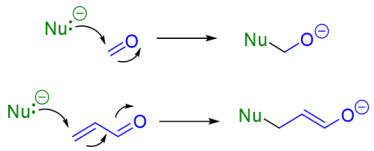

Table 6. Comparison of the Reactivities of the Cycloalkanones 1a–d toward Different Nucleophiles

	k_{CC}(**2b**)[a] (M^{-1} s^{-1})	k_2($NaBH_4$)[b] (M^{-1} s^{-1})	k_{rel}(**2b**)[a]	k_{rel}($NaBH_4$)[b]	k_{rel}(Nu)[c]
1a	1.33×10^4	2.66×10^{-2}	27	1.6	1.2
1b	2.14×10^2	7.01×10^{-4}	0.44	0.044	0.066
1c	4.85×10^2	1.61×10^{-2}	1	1	1
1d	3.88×10^1[d]	1.02×10^{-4}	0.080	0.0063	0.11

[a]In DMSO, 20 °C, from Table 2. [b]In *i*PrOH, 0 °C, from ref 4c. [c]Averaged value derived from reactions with NH_2OH, SO_3^{2-}, CN^-, BH_4^-, and $HOC_2H_4S^-$ in aqueous solution; $k_{rel}(Nu) = 10^B$ calculated from Geneste's *B* values defined by the relation $\log k = A \log k_0 + B$ in ref 5f. [d]From the rate constant with **2a** (Table 2) divided by 9.8, the reactivity ratio **2a**/**2b** toward cyclohexanone (**1c**).

observed in reactions with other nucleophiles, though the relative reactivities of the different cycloalkanones depend on the reaction partner and conditions.[39] The uniformly higher electrophilic reactivity of cyclobutanone (**1a**) can partially be explained by the higher release of ring strain during conversion of the sp^2 carbon in the four-membered ring into an sp^3 carbon. Table 5 shows, however, that the gas-phase methyl anion affinity of **1a** is only 5 kJ mol^{-1} higher than that of cyclohexanone (**1c**), indicating that release of strain can only account for part of the reactivity difference of **1a** and **1c**. Since the MAA of **1a** is almost 20 kJ mol^{-1} higher than that of **1c** in DMSO solution, we must conclude that differences of solvation are the major reason for the higher reactivity of cyclobutanone (**1a**) toward **2b** in solution. Let us analyze the origin of the solvation effect in the following comparison of cyclohexanone with cyclopentanone.

H. C. Brown rationalized the 23 times faster reaction of $NaBH_4$ with cyclohexanone compared to cyclopentanone by a change of torsional strain: As the hybridization of the carbonyl carbon changes from sp^2 to sp^3, the torsional strain increases in the five-membered ring (eclipsed bonds), but decreases in the six-membered ring because the equatorial hydrogens are nearly eclipsed with carbonyl oxygen in cyclohexanone and attain staggered arrangements in the chair conformation of cyclohexanol.[40] Since the opposite rehybridization takes place in the rate-determining step of S_N1 reactions of cycloalkyl halides, differences in torsional strain were analogously used to explain the much larger solvolysis rates of cyclopentyl halides compared to cyclohexyl halides.[40] We had already doubted that the change from C_{sp^3} to C_{sp^2} is the major contribution to this difference of the S_N1 reactivities because methylenecyclopentane was found to react 50 times faster with benzhydrylium ions than methylenecyclohexane though the rate-determining step does not involve rehybridization of a ring carbon.[41]

The 12.5 kJ mol^{-1} higher gas-phase methyl anion affinity of cyclohexanone (**1c**) compared to cyclopentanone (**1b**) in Table 5 supports the torsional strain argument. However, the difference between the MAAs of **1c** and **1b** shrinks to 2.9 kJ mol^{-1} in DMSO solution. As discussed in detail in Figures S24 and S25 (Supporting Information), this change is due to the fact that the cyclohexanolate conformer with oxygen in the axial position, which is most stable in the gas phase, is less efficiently solvated and becomes even less stable in DMSO solution than the conformer with equatorial oxygen. Thus, the overall poorer solvation of the cyclohexanolate ion accounts for the fact that the MAA of cyclohexanone, which is much higher than that of cyclopentanone in the gas phase, is only slightly higher in solution. The poor solvation of the cyclohexanolate anion with oxygen in the axial position analogously accounts for the finding (Table 5) that the MAAs of cyclobutanone and cyclohexanone differ only slightly in the gas phase (5 kJ mol^{-1}) but strongly in solution (20 kJ mol^{-1}).

As shown in Table 7, the introduction of electronegative elements in the 4-position of cyclohexanone leads to an increase of the electrophilic reactivity toward carbanion **2b** as well as toward BH_4^-. Possibly different solvation accounts for the fact that the relative reactivities in the two reaction series correlate only moderately. From the fact that the data for the four six-membered ring ketones **1c**, **1e**, **1f**, and **1g** are perfectly on the correlation line of Figure 10, one can conclude that the relative reactivities of these ketones are predominantly controlled by the thermodynamics of the CC-bond-forming step. Though oxygen is more electronegative than sulfur, tetrahydrothiopyranone (**1g**) is more electrophilic than tetrahydropyranone (**1f**), which may be due to through-bond interaction.[42]

Table 7. Influence of Heteroatoms in the γ-Position on the Reactivities of Cyclic Ketones

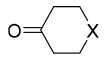

ketone **1**	k_{rel}(**2b**)[a]	k_{rel}(BH_4^-)[b]
1c (X = CH_2)	1.0	1.0
1e (X = NMe)	5.0	9.9
1f (X = O)	18	
1g (X = S)	59	11.2

[a]k_{CC} in DMSO from Table 2. [b]In water/dioxane (1/1) at 25 °C (from ref 5a).

When the β-carbon of ketones is replaced by sulfur (**1i** → **1j**) or oxygen (**1i** → **1k**), the heteroatom effect is larger (by a factor of 400 for S and not measurable for O) than the γ-heteroatom effect shown in Table 7 and follows the electronegativity order O ≫ S.

CONCLUSIONS

The arylsulfonyl-substituted chloromethyl anions **2a**,**b** are suitable reference nucleophiles for the determination of the electrophilic reactivities of ordinary aliphatic ketones. The rate constants k_{CC} for the initial nucleophilic attack are accessible by combination of the directly measured gross rate constants (k_2^{exptl}) for the formation of the epoxides **3** from the reactants **1** and **2** with the degree of reversibility of the initial step (k_{-CC}/k_{rc}). This ratio was derived from crossover experiments with the independently synthesized intermediates **4**. Two reaction pathways have been identified for the reactions of the carbanions **2** with the ketones **1**: one which yields the intermediate halohydrin anions **4** with the C–Cl and C–O^- bonds in *anti*-arrangements that can undergo direct cyclization to the epoxides **3** and a second one which gives the halohydrin

DOI: 10.1021/jacs.8b01657
J. Am. Chem. Soc. XXXX, XXX, XXX–XXX

anions **4** with C−Cl and C−O$^-$ in *gauche* orientation. The latter undergo retroaddition with regeneration of the reactants **1** and **2**, because the barrier for reversal is lower than the barrier for rotation to give the *anti* conformer suitable for cyclization. The cyclopropanation of diethyl maleate with **2a** proceeds via an analogous mechanism, with the difference that the initial CC-bond-forming step, which also gives different conformers, is irreversible.

The electrophilicity parameters E of the ketones **1** were calculated by eq 1 from the rate constants k_{CC} and the previously reported reactivity parameters N and s_N for the carbanions **2**. The E parameters, which refer to the nucleophilic attack of **2** at the carbonyl groups, correlate moderately with the gas-phase LUMO energies of the ketones (R^2 = 0.76, Figure 8), poorly with Parr's global electrophilicity index ω (R^2 = 0.61, Figure 9), very poorly with Parr's local electrophilicity index ω_C (R^2 = 0.30, Figure S33A in the Supporting Information), and best with the methyl anion affinities calculated for DMSO solution (R^2 = 0.87, Figure 10). We thus do not consider Parr's electrophilicity indices suitable measures for electrophilic reactivities, though electrophilic reactivities within a series of structurally closely related Michael acceptors correlate well with Parr's indices.[30]

Comparison of the electrophilicities E of ketones with those of Michael acceptors shows that ketones are significantly more electrophilic than Michael acceptors of equal methyl anion affinity (≙ Lewis acidity), indicating that nucleophilic additions to ketones proceed over much lower Marcus intrinsic barriers due to less electronic and geometrical reorganization than in Michael additions.

Crossover experiments showed that the initial attack of the *p*-cyanophenyl sulfonium ylide at aldehydes is reversible (in contrast to previous extrapolations), with the consequence that the previously reported E parameters for aldehydes correspond to the gross rate constants for these epoxidations and do not reflect the rates of initial attack of nucleophiles at the carbonyl group. By using the carbanions **2** as reference nucleophiles, estimates for the rate of nucleophilic attack at aldehydes have been obtained, showing that the electrophilicity parameter E of benzaldehyde (**1m**) is approximately 7 units greater than that of cyclohexanone (**1c**).

As illustrated in Figure 12, the electrophilicities of saturated aliphatic ketones are comparable to the C=C bond reactivities of *β*-phenyl-substituted *α,β*-unsaturated ketones and much lower than the C=C bond reactivities of terminally unsaturated vinyl ketones. Benzaldehyde, on the other hand, is more electrophilic than the *α,β*-unsaturated carbonyl compounds depicted in Figure 12, in line with the observation that *α,β*-unsaturated aldehydes usually undergo 1,2-additions under kinetically controlled conditions. In earlier applications of eq 1, we have shown that in reactions of nucleophiles with carbenium ions and a variety of Michael acceptors the electrophilicity parameters E can be treated as solvent-independent quantities, with the consequence that all solvent effects are shifted into the nucleophile-specific parameters N and s_N. Because of the high basicity of alkoxide ions in aprotic media, this approximation probably does not hold for the electrophilicities of carbonyl compounds, and systematic investigations of solvent effects are now needed to arrive at reliable predictions of carbonyl reactivities in different solvents.

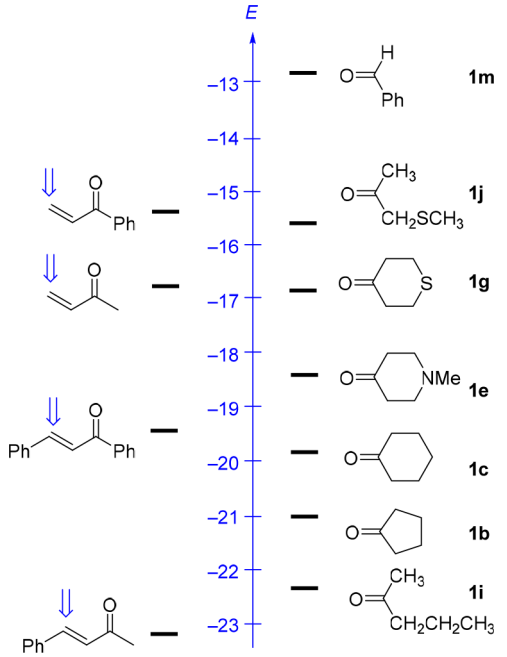

Figure 12. Comparison of the empirical electrophilicities E of carbonyl groups and Michael acceptors in DMSO.

■ ASSOCIATED CONTENT

Supporting Information

The Supporting Information is available free of charge on the ACS Publications website at DOI: 10.1021/jacs.8b01657.

Details of the product studies, kinetic experiments, NMR spectra of all characterized compounds, single-crystal X-ray structure of **4ca**-H, competition experiments, crossover experiments, and computational analysis (PDF)
Coordinates of optimized structures (ZIP)
Crystallographic data for **4ca**-H (CIF)

■ AUTHOR INFORMATION

Corresponding Authors

*ofial@lmu.de
*zipse@cup.uni-muenchen.de
*herbert.mayr@cup.uni-muenchen.de

ORCID

Armin R. Ofial: 0000-0002-9600-2793
Hendrik Zipse: 0000-0002-0534-3585
Herbert Mayr: 0000-0003-0768-5199

Notes

The authors declare no competing financial interest.

■ ACKNOWLEDGMENTS

This paper is dedicated to Professor Ernst-Ulrich Würthwein on the occasion of his 70th birthday. We thank the Deutsche Forschungsgemeinschaft (SFB 749, Projects B1 and C6) and the China Scholarship Council (fellowship to Z.L.) for financial support. We are grateful for computing time on the Linux-Cluster at the Leibniz Supercomputing Centre (www.lrz.de) and thank Dr. Peter A. Byrne (University College Cork, Ireland) for helpful discussions.

DOI: 10.1021/jacs.8b01657
J. Am. Chem. Soc. XXXX, XXX, XXX−XXX

REFERENCES

(1) (a) Mayr, H.; Bug, T.; Gotta, M. F.; Hering, N.; Irrgang, B.; Janker, B.; Kempf, B.; Loos, R.; Ofial, A. R.; Remennikov, G.; Schimmel, H. *J. Am. Chem. Soc.* **2001**, *123*, 9500−9512. (b) Lucius, R.; Loos, R.; Mayr, H. *Angew. Chem., Int. Ed.* **2002**, *41*, 91−95. (c) Mayr, H.; Kempf, B.; Ofial, A. R. *Acc. Chem. Res.* **2003**, *36*, 66−77.

(2) Appel, R.; Mayr, H. *J. Am. Chem. Soc.* **2011**, *133*, 8240−8251.

(3) (a) Zimmerman, H. E.; Ahramjian, L. *J. Am. Chem. Soc.* **1960**, *82*, 5459−5466. (b) Vogt, P. F.; Tavares, D. F. *Can. J. Chem.* **1969**, *47*, 2875−2881. (c) Aggarwal, V. K.; Calamai, S.; Ford, J. G. *J. Chem. Soc., Perkin Trans. 1* **1997**, 593−599.

(4) (a) Brown, H. C.; Mead, E. J.; Rao, B. C. S. *J. Am. Chem. Soc.* **1955**, *77*, 6209−6213. (b) Brown, H. C.; Wheeler, O. H.; Ichikawa, K. *Tetrahedron* **1957**, *1*, 214−220. (c) Brown, H. C.; Ichikawa, K. *Tetrahedron* **1957**, *1*, 221−230. (d) Brown, H. C.; Ichikawa, K. *J. Am. Chem. Soc.* **1962**, *84*, 373−376. (e) Brown, H. C.; Muzzio, J. *J. Am. Chem. Soc.* **1966**, *88*, 2811−2822. (f) Brown, H. C.; Wang, K. K.; Chandrasekharan, J. *J. Am. Chem. Soc.* **1983**, *105*, 2340−2343.

(5) (a) Geneste, P.; Durand, R.; Hugon, I.; Reminiac, C. *J. Org. Chem.* **1979**, *44*, 1971−1973. (b) Geneste, P.; Lamaty, G.; Moreau, C.; Roque, J. P. *Tetrahedron Lett.* **1970**, *11*, 5011−5014. (c) Geneste, P.; Lamaty, G.; Roque, J. P. *Tetrahedron* **1971**, *27*, 5539−5559. (d) Geneste, P.; Lamaty, G.; Roque, J. P. *Tetrahedron* **1971**, *27*, 5561−5578. (e) Fournier, L.; Lamaty, G.; Natat, A.; Roque, J. P. *Tetrahedron* **1975**, *31*, 1031−1034. (f) Finiels, A.; Geneste, P. *J. Org. Chem.* **1979**, *44*, 1577−1578.

(6) (a) Zenz, I.; Mayr, H. *J. Org. Chem.* **2011**, *76*, 9370−9378. (b) Kaumanns, O.; Lucius, R.; Mayr, H. *Chem. - Eur. J.* **2008**, *14*, 9675−9682. (c) Lemek, T.; Mayr, H. *J. Org. Chem.* **2003**, *68*, 6880−6886. (d) For a comprehensive database of nucleophilicity parameters *N* and s_N as well as electrophilicity parameters *E*, see http://www.cup.lmu.de/oc/mayr/DBintro.html.

(7) (a) Olmstead, W. N.; Margolin, Z.; Bordwell, F. G. *J. Org. Chem.* **1980**, *45*, 3295−3299. (b) Bordwell, F. G. *Acc. Chem. Res.* **1988**, *21*, 456−463.

(8) (a) Arnett, E. M.; Maroldo, S. G.; Schilling, S. L.; Harrelson, J. A. *J. Am. Chem. Soc.* **1984**, *106*, 6759−6767. (b) For a comprehensive list of pK_a values, see http://ibond.nankai.edu.cn/.

(9) (a) Darzens, G. *Compt. Rend.* **1904**, *139*, 1214−1217. (b) Darzens, G. *Compt. Rend.* **1905**, *141*, 766−768. (c) Darzens, G. *Compt. Rend.* **1906**, *142*, 214−215. (d) Darzens, G.; Lefébure, P. *Compt. Rend.* **1906**, *142*, 714−715.

(10) (a) Newman, M. S.; Magerlein, B. J. *Org. React.* **1949**, *5*, 413−440. (b) Rosen, T. Darzens Glycidic Ester Condensation. In *Comprehensive Organic Synthesis*, 1st ed.; Trost, B. M., Fleming, I., Eds.; Pergamon Press: Oxford, U.K., 1991; Vol. *2*, pp 409−439. (c) Aggarwal, V. K.; Crimmin, M.; Riches, S. Synthesis of Epoxide by Carbonyl Epoxidation. In *Science of Synthesis*; Forysth, C. J., Jacobsen, E. N., Eds.; Thieme: Stuttgart, Germany, 2008; Vol. *37*, pp 321−406. (d) Reutrakul, V.; Pohmakotr, M. Chloromethyl Phenyl Sulfone. In *Encyclopedia of Reagents for Organic Synthesis*, 2nd ed.; Paquette, L. A., Crich, D., Fuchs, P. L., Molander, G. A., Eds.; Wiley: Chichester, U.K., 2009; Vol. *4*, pp 2375−2378. (e) Bako, P.; Rapi, Z.; Keglevich, G. *Curr. Org. Synth.* **2014**, *11*, 361−376. For diastereoselective or asymmetric Darzens reactions, see: (f) Liu, Y.; Provencher, B. A.; Bartelson, K. J.; Deng, L. *Chem. Sci.* **2011**, *2*, 1301−1304. (g) Kuang, Y.; Lu, Y.; Tang, Y.; Liu, X.; Lin, L.; Feng, X. *Org. Lett.* **2014**, *16*, 4244−4247. (h) Li, B.; Li, C. *J. Org. Chem.* **2014**, *79*, 8271−8277. (i) Sakowicz, A.; Loska, R.; Mąkosza, M. *Synlett* **2016**, *27*, 2443−2446. (j) Chai, G.-L.; Han, J.-W.; Wong, H. N. C. *Synthesis* **2017**, *49*, 181−187. (k) Chai, G.-L.; Han, J.-W.; Wong, H. N. C. *J. Org. Chem.* **2017**, *82*, 12647−12654.

(11) Ballester, M. *Chem. Rev.* **1955**, *55*, 283−300.

(12) (a) Bachelor, F. W.; Bansal, R. K. *J. Org. Chem.* **1969**, *34*, 3600−3604. (b) Sipos, G.; Schöbel, G.; Sirokmán, F. *J. Chem. Soc., Perkin Trans. 2* **1975**, 805−808.

(13) (a) Corey, E. J.; Chaykovsky, M. *J. Am. Chem. Soc.* **1965**, *87*, 1353−1363. (b) Johnson, A. W.; LaCount, R. B. *J. Am. Chem. Soc.* **1961**, *83*, 417−423.

(14) (a) Aggarwal, V. K.; Winn, C. L. *Acc. Chem. Res.* **2004**, *37*, 611−620. (b) McGarrigle, E. M.; Myers, E. L.; Illa, O.; Shaw, M. A.; Riches, S. L.; Aggarwal, V. K. *Chem. Rev.* **2007**, *107*, 5841−5883.

(15) (a) Appel, R.; Mayr, H. *Chem. - Eur. J.* **2010**, *16*, 8610−8614. (b) Appel, R.; Hartmann, N.; Mayr, H. *J. Am. Chem. Soc.* **2010**, *132*, 17894−17900.

(16) Li, Z.; Chen, Q.; Mayer, P.; Mayr, H. *J. Org. Chem.* **2017**, *82*, 2011−2017.

(17) Mayr, H.; Ofial, A. R. *Angew. Chem., Int. Ed.* **2006**, *45*, 1844−1854.

(18) Schwesinger, R.; Schlemper, H.; Hasenfratz, C.; Willaredt, J.; Dambacher, T.; Breuer, T.; Ottaway, C.; Fletschinger, M.; Boele, J.; Fritz, H.; Putzas, D.; Rotter, H. W.; Bordwell, F. G.; Satish, A. V.; Ji, G. Z.; Peters, E. M.; Peters, K.; von Schnering, H. G.; Walz, L. *Liebigs Ann.* **1996**, 1055−1081.

(19) (a) Durst, T.; Tin, K.-C.; De Reinach-Hirtzbach, F.; Decesare, J. M.; Ryan, M. D. *Can. J. Chem.* **1979**, *57*, 258−266. (b) Reutrakul, V.; Jarussophon, S.; Pohmakotr, M.; Chaiyasut, Y.; U-Thet, S.; Tuchinda, P. *Tetrahedron Lett.* **2002**, *43*, 2285−2288.

(20) Arai, S.; Shioiri, T. *Tetrahedron* **2002**, *58*, 1407−1413.

(21) Becke, A. D. *J. Chem. Phys.* **1993**, *98*, 5648−5652.

(22) (a) Grimme, S. *J. Comput. Chem.* **2006**, *27*, 1787−1799. (b) Grimme, S.; Antony, J.; Ehrlich, S.; Krieg, H. *J. Chem. Phys.* **2010**, *132*, 154104. (c) Wagner, J. P.; Schreiner, P. R. *Angew. Chem., Int. Ed.* **2015**, *54*, 12274−12296.

(23) (a) Ditchfield, R.; Hehre, W. J.; Pople, J. A. *J. Chem. Phys.* **1971**, *54*, 724−728. (b) Krishnan, R.; Binkley, J. S.; Seeger, R.; Pople, J. A. *J. Chem. Phys.* **1980**, *72*, 650−654.

(24) (a) Cancès, E.; Mennucci, B.; Tomasi, J. *J. Chem. Phys.* **1997**, *107*, 3032−3041. (b) Tomasi, J.; Mennucci, B.; Cammi, R. *Chem. Rev.* **2005**, *105*, 2999−3094. (c) Mayer, R. J.; Tokuyasu, T.; Mayer, P.; Gomar, J.; Sabelle, S.; Mennucci, B.; Mayr, H.; Ofial, A. R. *Angew. Chem., Int. Ed.* **2017**, *56*, 13279−13282.

(25) Grimme, S. *J. Chem. Phys.* **2006**, *124*, 034108.

(26) (a) Weigend, F.; Ahlrichs, R. *Phys. Chem. Chem. Phys.* **2005**, *7*, 3297−3305. (b) Weigend, F. *Phys. Chem. Chem. Phys.* **2006**, *8*, 1057−1065.

(27) The corresponding competition experiment with **2b** could not be performed because of the low stability of the resulting oxiranes.

(28) Huisgen, R. *Angew. Chem., Int. Ed. Engl.* **1970**, *9*, 751−762.

(29) (a) Allgäuer, D. S.; Jangra, H.; Asahara, H.; Li, Z.; Chen, Q.; Zipse, H.; Ofial, A. R.; Mayr, H. *J. Am. Chem. Soc.* **2017**, *139*, 13318−13329. (b) Mayr, H.; Ammer, J.; Baidya, M.; Maji, B.; Nigst, T. A.; Ofial, A. R.; Singer, T. *J. Am. Chem. Soc.* **2015**, *137*, 2580−2599.

(30) Domingo, L. R.; Pérez, P.; Contreras, R. *Tetrahedron* **2004**, *60*, 6585−6591.

(31) (a) Contreras, R. R.; Fuentealba, P.; Galván, M.; Pérez, P. *Chem. Phys. Lett.* **1999**, *304*, 405−413. (b) Yang, W.; Mortier, W. J. *J. Am. Chem. Soc.* **1986**, *108*, 5708−5711.

(32) Clark, T.; Chandrasekhar, J.; Spitznagel, G. W.; Schleyer, P. v. R. *J. Comput. Chem.* **1983**, *4*, 294−301.

(33) Marenich, A. V.; Cramer, C. J.; Truhlar, D. G. *J. Phys. Chem. B* **2009**, *113*, 6378−6396.

(34) (a) Wang, C.; Fu, Y.; Guo, Q.-X.; Liu, L. *Chem. - Eur. J.* **2010**, *16*, 2586−2598. (b) Zhuo, L.-G.; Liao, W.; Yu, Z.-X. *Asian J. Org. Chem.* **2012**, *1*, 336−345.

(35) (a) Aizman, A.; Contreras, R.; Pérez, P. *Tetrahedron* **2005**, *61*, 889−895. (b) Pérez, P.; Domingo, L. R.; Aizman, A.; Contreras, R. In *Theoretical Aspects of Chemical Reactivity*; Toro-Labbé, A., Ed.; Theoretical and Computational Chemistry, Vol. *19*; Elsevier: Amsterdam, 2007; Chapter 9, pp 139−201. (c) Chamorro, E.; Duque-Noreña, M.; Pérez, P. *J. Mol. Struct.: THEOCHEM* **2009**, *896*, 73−79. (d) Chamorro, E.; Duque-Noreña, M.; Pérez, P. *J. Mol. Struct.: THEOCHEM* **2009**, *901*, 145−152.

(36) Byrne, P. A.; Kobayashi, S.; Würthwein, E.-U.; Ammer, J.; Mayr, H. *J. Am. Chem. Soc.* **2017**, *139*, 1499−1511.

(37) $\Delta\Delta G^{\ddagger} = 2.303RT[\Delta(\log k)] = 2.303RTs_N\Delta E$.

(38) (a) Marcus, R. A. *J. Chem. Phys.* **1956**, *24*, 966−978. (b) Marcus, R. A. *J. Phys. Chem.* **1968**, *72*, 891−899. (c) Albery, W. J. *Annu. Rev.*

DOI: 10.1021/jacs.8b01657
J. Am. Chem. Soc. XXXX, XXX, XXX−XXX

Phys. Chem. **1980**, *31*, 227−263. (d) Murdoch, J. R.; Magnoli, D. E. *J. Am. Chem. Soc.* **1982**, *104*, 3792−3800. (e) Chen, M. Y.; Murdoch, J. R. *J. Am. Chem. Soc.* **1984**, *106*, 4735−4743. (f) Hine, J. *Adv. Phys. Org. Chem.* **1977**, *15*, 1−61.

(39) Carey, F. A., Sundberg, R. J. *Advanced Organic Chemistry Part A: Structure and Mechanisms*, 5th ed; Springer: New York, 2007; pp 632−637.

(40) Brown, H. C.; Borkowski, M. *J. Am. Chem. Soc.* **1952**, *74*, 1894−1902.

(41) Roth, M.; Schade, C.; Mayr, H. *J. Org. Chem.* **1994**, *59*, 169−172.

(42) Hoffmann, R. *Acc. Chem. Res.* **1971**, *4*, 1−9.

DOI: 10.1021/jacs.8b01657
J. Am. Chem. Soc. XXXX, XXX, XXX−XXX